

**The Air Pollution Model (TAPM) Version 3.  
Part 2: Summary of Some Verification  
Studies.**

**Peter J. Hurley, William L. Physick, Ashok K. Luhar  
and Mary Edwards**



**CSIRO**

---

**Atmospheric Research**

CSIRO Atmospheric Research Technical Paper 72

**The Air Pollution Model (TAPM) Version 3.  
Part 2: Summary of Some Verification Studies**

Peter J. Hurley, William L. Physick, Ashok K. Luhar and Mary Edwards

**The National Library of Australia Cataloguing-in-Publication entry**

The air pollution model (TAPM) version 3. Part 2, Summary of some verification studies.

ISBN 0 643 06653 5.

1. Air - Pollution - Mathematical models. 2. Air - Pollution - Measurement. 3. Air - Pollution - Meteorological aspects. I. Hurley, Peter, 1963- . II. CSIRO. Division of Atmospheric Research. (Series : CSIRO Atmospheric Research technical paper (Online) ; 72).

363.7392

Address and contact details: CSIRO Atmospheric Research  
Private Bag No. 1 Aspendale Victoria 3195 Australia  
Ph: (+61 3) 9239 4400; fax: (+61 3) 9239 4444  
e-mail: [ar-enquiries@csiro.au](mailto:ar-enquiries@csiro.au)

CSIRO Atmospheric Research Technical Papers may be issued out of sequence. From July 2000 All new Technical Papers will appear on the web site of CSIRO Atmospheric Research. Some Technical Papers will also appear in paper form.

© CSIRO Australia – Electronic edition 2005

## **The Air Pollution Model (TAPM) Version 3. Part 2: Summary of Some Verification Studies.**

Peter J. Hurley, William L. Physick, Ashok K. Luhar and Mary Edwards  
CSIRO Atmospheric Research  
Private Bag 1, Aspendale,  
Vic. 3195, Australia

### **Abstract**

Air pollution predictions for environmental impact assessments usually use Gaussian plume/puff models driven by observationally-based meteorological inputs. An alternative approach is to use prognostic meteorological and air pollution models, which have many advantages over the Gaussian approach and have now become a viable tool for performing year-long simulations. Continuing rapid increases in computing power have brought this approach well within the reach of a desktop PC. This paper provides some verification studies of The Air Pollution Model (TAPM) for a number of laboratory experiments of dispersion, for two US tracer experiments (Kincaid and Indianapolis) used internationally for model inter-comparison studies, and for meteorology and/or dispersion in various regions throughout Australia (Anglesea, Kwinana, Kalgoorlie, the Pilbara and Melbourne).

The meteorological results show that TAPM performs well in a variety of regions throughout Australia (e.g., coastal, inland and generally complex terrain for sub-tropical to mid-latitude conditions). The pollution results show that TAPM performs well for a range of important phenomena (e.g. concentration variance and fluctuation intensity; building wakes; nocturnal inversion break-up fumigation; stable, neutral, and convective dispersion; shoreline fumigation; and general dispersion in complex rural and urban conditions). In particular, TAPM performs very well for the prediction of extreme pollution statistics, important for environmental impact assessments, for both non-reactive (tracer) and reactive (nitrogen dioxide, ozone and particulate) pollutants for a variety of sources (e.g. industrial stacks and/or general surface or urban emissions).

## **1 Introduction**

Air pollution models that can be used to predict pollution concentrations for periods of up to a year are generally semi-empirical/analytic approaches based on Gaussian plumes or puffs. These models typically use either a simple surface-based meteorological file or a diagnostic wind field model based on available observations. The Air Pollution Model (TAPM – see Hurley et al., 2005b, for details on TAPM V2) is different to these approaches in that it solves the fundamental fluid dynamics and scalar transport equations to predict meteorology and pollutant concentration for a range of pollutants important for air pollution applications. It consists of coupled prognostic meteorological and air pollution concentration components, eliminating the need to have site-specific meteorological observations. Instead, the model predicts the flows important to local-scale air pollution, such as sea breezes and terrain-induced flows, against a background of larger-scale meteorology provided by synoptic analyses.

This paper follows on from the technical description of the model (TAPM V3) in part 1 of this series (Hurley, 2005), and updates and summarises a number of model verification studies presented previously in the literature, that used earlier versions of the model (e.g. TAPM V2). Section 2 compares TAPM predictions with results from laboratory experiments of point source dispersion in the convective boundary layer and within building wakes. In Section 3, TAPM is verified for two US tracer datasets (Kincaid and Indianapolis) used for international model inter-comparison. Sections 4 and 5 present model verification for the Anglesea (Victoria) and Kwinana (Western Australia) regions for annual datasets of sulfur dioxide dispersion. Section 6 examines the performance of the model for upper-level meteorology, by comparing wind predictions to SODAR data for the Kalgoorlie region. Sections 7 and 8 look at annual meteorology and photochemically reactive dispersion, for point sources in the Pilbara (Western Australia), and for urban sources in Melbourne (Victoria). All of these verification datasets have well known emission characteristics and good quality monitoring data with well quantified uncertainties, allowing a meaningful evaluation of model performance to be made.

## 2 Comparison of TAPM with dispersion data from laboratory experiments

This Section compares TAPM Version 3 (V3) predictions with results from laboratory experiments of point source dispersion in the convective boundary layer (concentration fluctuation intensity) and for point source dispersion within building wakes.

### 2.1 Dispersion in the Convective Boundary Layer – Fluctuation Intensity

As described in part 1 of this series (Hurley, 2005) the Lagrangian particle approach has been previously well verified against laboratory data of dispersion in the convective boundary layer. Here we extend this verification to look at the performance of the concentration fluctuation intensity – the ratio of the square root of the concentration variance divided by the mean concentration.

TAPM was run using a synoptic wind speed of  $5 \text{ m s}^{-1}$  and a typical temperature/moisture profile. TAPM pollution was configured with a non-buoyant point source at a height of 300 m, and was run in Lagrangian mode with concentration variance switched-on. Results were extracted during the mid-afternoon when the mixing height had reached an approximate steady-state value of 1500 m. Sensitivity runs showed that the non-dimensional results were not very sensitive to the synoptic inputs or to the source height.

Figure 2.1 shows the variation of predicted and observed concentration fluctuation intensity with convectively scaled downwind distance ( $X$ ) at ground level. The results show that the observed fluctuation intensity data from Deardorff and Willis (1984) are predicted very well, with the model curve showing correct behaviour for all distances downwind. Note that at small downwind distance ( $X < 0.5$ ) where observations are not available, the model shows the expected behaviour of high intensity near the (leading) edge of the plume (where mean concentration is small).

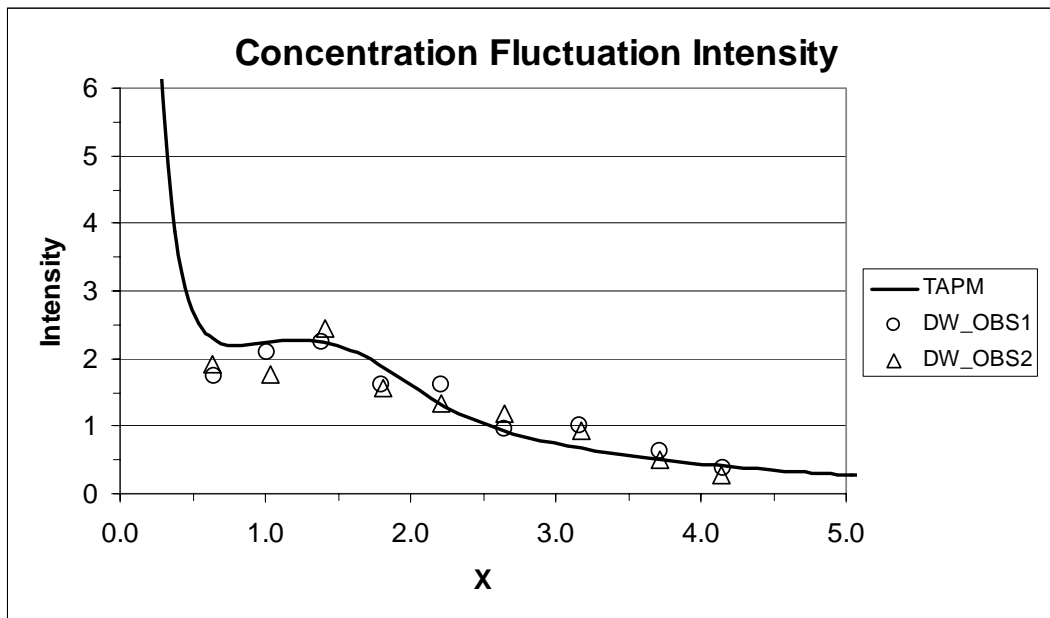


Figure 2.1. Predicted (TAPM) and observed concentration fluctuation intensity at ground level. Note that DW\_OBS1 data are averaged over  $0.5 < |Y| < 1.0$  and DW\_OBS2 data are averaged over  $|Y| < 0.5$ , whereas TAPM is for the plume centreline. ( $Y$  is the plume lateral distance from the centreline divided by the standard deviation of the plume width).

## 2.2 Dispersion in building wakes

The effect of building wakes on plume rise and dispersion in TAPM is based on the Plume Rise Model Enhancements (PRIME) approach of Schulman *et al.* (2000). The PRIME model uses an along-wind coordinate system, and so first each building is transformed to be in this system. Effective building dimensions and cavity and wake dimensions are then calculated for each building, which are used to determine the combined wake meteorology and turbulence. Plume rise and dispersion are affected by the modified meteorology and turbulence for point sources in both EGM (Eulerian Grid Module) and LPM (Lagrangian Grid Module) modes. LPM calculations are done for both the cavity and wake regions, rather than specifying a uniform concentration in the cavity as is done in PRIME.

Here TAPM is used in LPM mode to simulate point source dispersion in a single building wake for the wind tunnel experiments of Thompson (1993). These data provide an independent test of the building wake algorithms, as they have not been used in the development of PRIME, and represent point source dispersion for non-buoyant sources in the near-wake or cavity region for four different building shapes. Schulman *et al.* (2000) also used PRIME and ISC3 to simulate one of the building shapes used by Thompson (1993), while the equation for maximum (uniform) cavity concentration for both of these models has been used here for the remaining building shapes. The model was run with flat terrain in a nested, non-time varying synoptic mode, assimilating a uniform wind speed profile over the lowest 300 m, with a pollution inner grid spacing of 50 m. The dimensions of the four buildings used were:

- BLD1:  $W = H$  and  $L = H$ ;
- BLD2:  $W = 2H$  and  $L = H$ ;
- BLD3:  $W = 4H$  and  $L = H$ ;
- BLD4:  $W = H$  and  $L = 2H$ ;

where  $W$  = building width,  $L$  = building length,  $H$  = building height, and here we have used  $H = 100$  m. The stack height for the point source was  $H_S = 0.5H$ , located at one stack height downwind of the centre of the lee face of the building (i.e., at downwind distance  $X = H$ , and crosswind distance  $Y = 0$ ).

Non-dimensional plume centreline ground level concentrations as a function of downwind distance are shown in Figure 2.2 for both observations and model predictions for BLD1 (observations, and predictions by both PRIME and ISC3, are taken from Schulman *et al.*, 2000). The results show that TAPM predicts the maximum cavity concentration very well, but tends to underestimate the concentration behind the source (between the building and the stack), while PRIME underestimates the maximum, but represents the concentration behind the source well, and ISC3 significantly underestimates the cavity concentration. All models do a reasonable job in the far-wake region from about  $X = 4H$  onwards.

The maximum cavity concentrations have also been calculated for all models for each of the four building shapes and the results are shown in Figure 2.3. The results show that TAPM performs well in representing both the magnitude and the variation of the maximum cavity concentration with building shape. PRIME also does a good job for BLD3 and BLD4, but tends to underestimate the maximum cavity concentration for BLD1 and particularly for BLD2. ISC3 has a similar variation of maximum cavity concentration as for PRIME, but the magnitude is much too low.

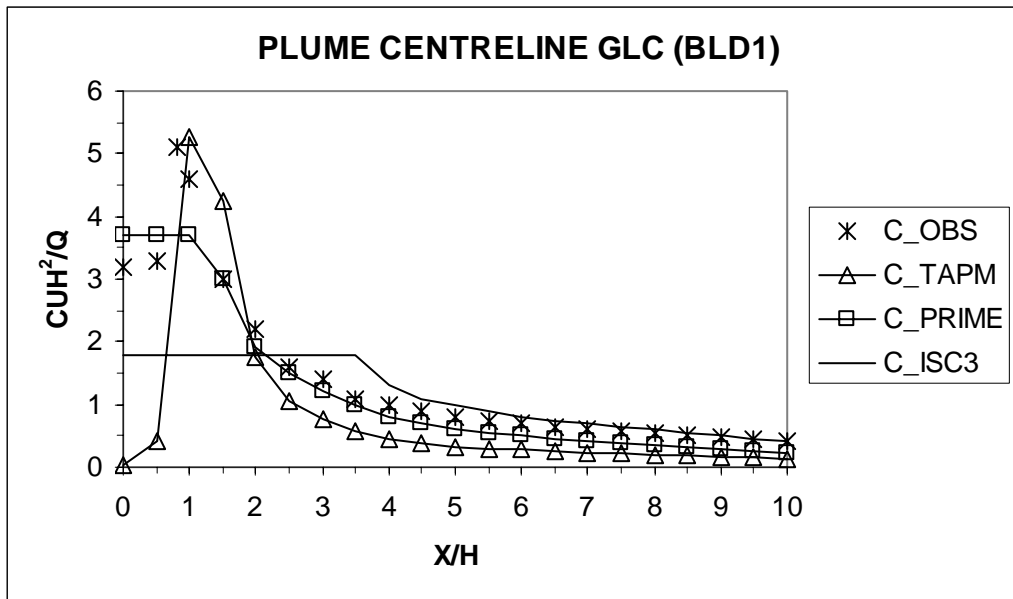


Figure 2.2. Observed (OBS) and predicted (TAPM, PRIME and ISC3) plume centreline ground level concentration (GLC), downwind of BLD1.

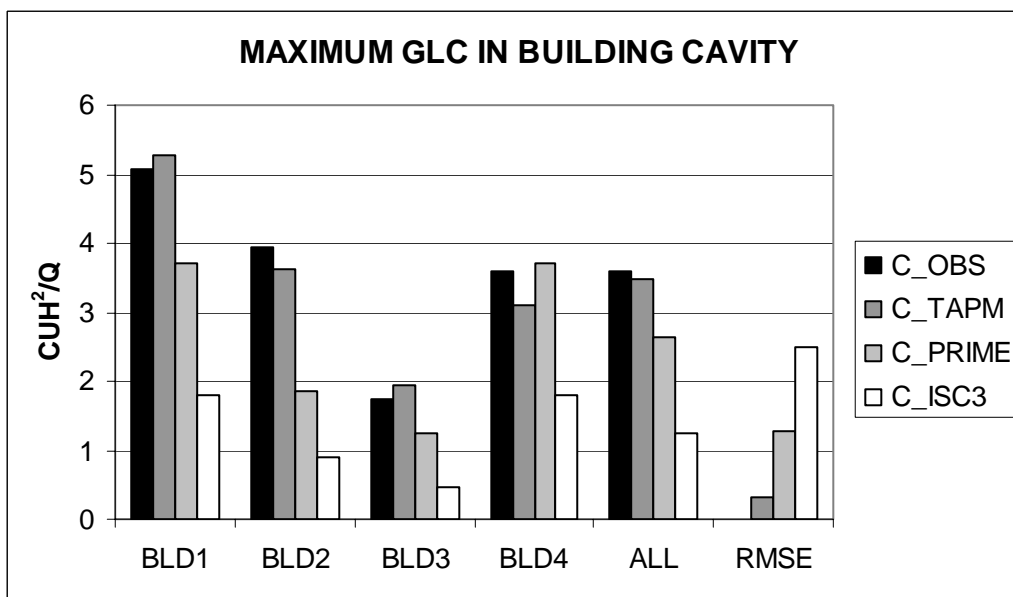


Figure 2.3. Observed (OBS) and predicted (TAPM, PRIME and ISC3) maximum plume centreline ground level concentration (GLC), for BLD1, BLD2, BLD3, BLD4, and the average (ALL) and root mean square error (RMSE) over all buildings.

### 3 International model inter-comparison datasets

In 1991, The Joint Research Centre of the European Commission launched an initiative for increased cooperation and standardisation of atmospheric dispersion models for regulatory purposes. As part of the initiative, a series of conferences on “Harmonisation within Atmospheric Dispersion Modelling for Regulatory Purposes” was organised to promote the use of new-generation models within atmospheric dispersion modelling, and in general improve “modelling culture” (for more details see Olesen, 1995). A set of four short-range field data sets, called the Model Validation Kit, was prepared to facilitate a standard and uniform comparison of model results. The two most comprehensive of the four field datasets on point-source plume dispersion are the 1980–81 Kincaid (rural) dataset, and the 1985 Indianapolis (urban) dataset, both taken in the US and widely used for model evaluation purposes. These two datasets were taken in relatively simple orography (i.e. flat terrain, no coastal influences), where simple plume models should be expected to perform well.

In this Section, the performance of TAPM V3 is evaluated for the Kincaid and Indianapolis datasets. TAPM was run with and without wind data assimilation – for more detail, see Luhar and Hurley (2003) and Hurley and Luhar (2005).

Since the above two data sets precede the global synoptic meteorological data supplied with TAPM, which are given from 1997, we used the National Center for Environmental Prediction (NCEP)/National Center for Atmospheric Research (NCAR) reanalysis data (Kalnay et al., 1996) on horizontal wind components, temperature and moisture, to obtain the required synoptic fields for the model. These data have a horizontal resolution of  $2.5^\circ$  and a temporal resolution of 6 h, while the vertical levels are in a pressure coordinate system with the lowest five levels being 1000, 925, 850, 700 and 600 hPa.

#### 3.1 Kincaid

EPRI’s (Electric Power Research Institute) Kincaid field study was conducted in 1980 and 1981 (Bowne et al., 1983). It involved sulfur hexafluoride ( $\text{SF}_6$ ) tracer releases from the 187 m stack (with diameter 9 m) at the Kincaid power plant in Illinois, USA ( $89.49^\circ\text{W}$ ,  $39.59^\circ\text{N}$ ). The power plant is surrounded by relatively flat farmland with some lakes (roughness length of about 0.1 m).

Most meteorological measurements were taken from 10-m and 100-m towers located on a central site about 650 m east of the power plant together with solar and terrestrial radiation measurement gear. The wind observations were taken at the 10, 30, 50 and 100 m AGL levels, while the temperature measurements were taken at the 10, 50 and 100 m levels. There are also data from a National Weather Service station 30.6 km northwest of the source, and profiles from routine radiosonde releases 120 km north of the source.

Hourly-averaged concentrations of  $\text{SF}_6$  due to buoyant power station plumes were observed by ground-level monitors on a maximum of 12 arcs at distances 0.5, 1, 2, 3, 5, 7, 10, 15, 20, 30, 40 and 50 km from the stack. There are three measurement periods: 20 April–9 May 1980, 10–25 July 1980, and 16 May–1 June 1981. Figure 3.1 shows the locations of the stack, meteorological sites and the tracer monitors on 22 May 1981. A total of 171 hours of tracer data are available in the Model Validation Kit, representing mostly daytime convective cases. Arc-wise maxima were calculated from the crosswind concentration variation, and a quality indicator was assigned to each value. It is recommended that only the data with quality indicator 2 (maxima identified) and 3 (maxima well defined) be used for model comparison. Out of a total of 1284 arc-hours of data, 585 are quality 2 and 3, and 338 are quality 3.

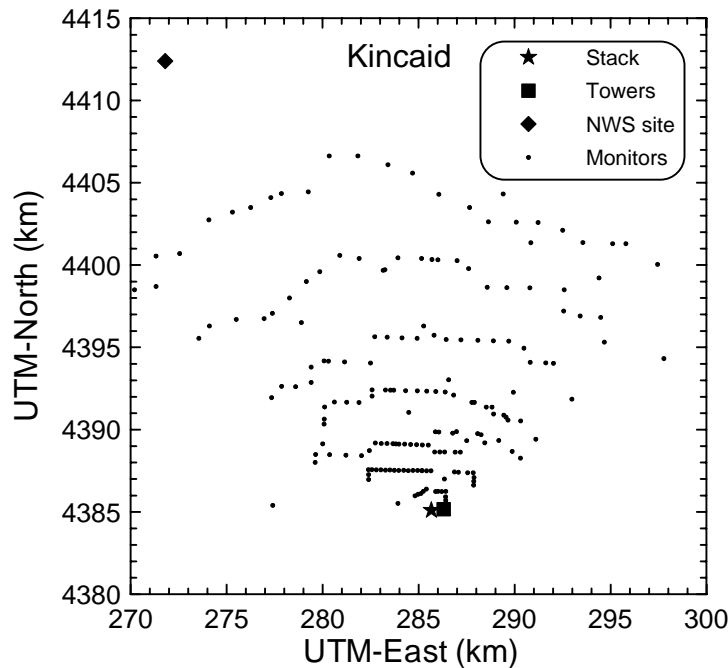


Figure 3.1. Concentration monitors (22 May 1981), and meteorological sites for the Kincaid study.

TAPM V3 was run for the above three data periods separately with an extra spin-up day at the start in each run. Three nested domains of  $31 \times 31$  horizontal grid points at 16-km, 4-km, and 1-km spacing for the meteorology, and  $61 \times 61$  horizontal grid points at 8-km, 2-km, and 0.5-km spacing for the pollution, both centred on the stack coordinates, were used. There were 25 vertical levels: 10, 25, 50, 100, 150, 200, 250, 300, 400, 500, 600, 750, 1000, 1250, 1500, 1750, 2000, 2500, 3000, 3500, 4000, 5000, 6000, 7000 and 8000 m. The model was run in Lagrangian mode to capture the near-source dispersion more accurately. Given that no advice based on local measurements was given about surface moisture availability, we used a deep soil moisture content of  $0.1 \text{ kg kg}^{-1}$ , which is a typical value used for summer conditions in rural areas. The wind speeds and directions observed at the tower site at four levels, namely 10, 30, 50 and 100 m AGL, were assimilated in model calculations. The hourly average pollution predictions on the 0.5 km spaced grid were processed to obtain ground-level concentration maxima at the 0.5, 1, 2, 3, 5, 7, 10 and 15 km arcs while those on the 2-km spaced pollution grid were processed to obtain the maxima at the 20, 30, 40 and 50 km arcs.

Table 3.1 lists model performance statistics for TAPM (with wind data assimilation) and TAPM-NA (without wind data assimilation), including  $\text{RHC}_R$  and  $\text{MAX}_R$  that indicate performance for the extreme end of the concentration distribution. The results show that TAPM performs well for both the mean and for the extreme performance statistics for the Kincaid dataset, with TAPM-NA also performing well, but slightly worse than TAPM for MEAN and slightly better for  $\text{RHC}_R$ .

Figure 3.2 shows TAPM Quantile-Quantile (Q-Q) plots of the (sorted) predicted versus the (sorted) observed concentrations for both Quality 2&3 and Quality 3 data. These plots again illustrate that TAPM performs well for extreme concentrations, and does slightly better for the higher quality data.

Table 3.1. Model performance statistics for Kincaid (a) for Quality 2&3 data and (b) for Quality 3 data. TAPM – with wind data assimilation. TAPM-NA – without wind data assimilation.

(a) Q2&3	MEAN	STD	NMSE	COR	IOA	RHC <sub>R</sub>	MAX <sub>R</sub>
<b>Observed</b>	41.0	39.3	0.0	1.00	1.00	1.00	1.00
<b>TAPM</b>	54.2	50.9	1.4	0.30	0.53	1.25	1.23
<b>TAPM-NA</b>	67.4	51.6	1.4	0.24	0.47	1.08	1.21

(b) Q3	MEAN	STD	NMSE	COR	IOA	RHC <sub>R</sub>	MAX <sub>R</sub>
<b>Observed</b>	54.3	40.3	0.0	1.00	1.00	1.00	1.00
<b>TAPM</b>	57.1	47.5	0.8	0.36	0.60	0.89	0.84
<b>TAPM-NA</b>	70.1	48.8	0.8	0.26	0.52	1.00	0.77

Key: MEAN = Arithmetic Mean ( $\text{ng m}^{-3} (\text{g s}^{-1})^{-1}$ ), STD = Standard Deviation ( $\text{ng m}^{-3} (\text{g s}^{-1})^{-1}$ ), NMSE = normalised mean square error, COR = correlation coefficient, IOA = Index of Agreement; RHC<sub>R</sub> = Ratio (Predicted/Observed) of Robust Highest Concentration (RHC); MAX<sub>R</sub> = Ratio (Predicted/Observed) of Maximum Concentration.

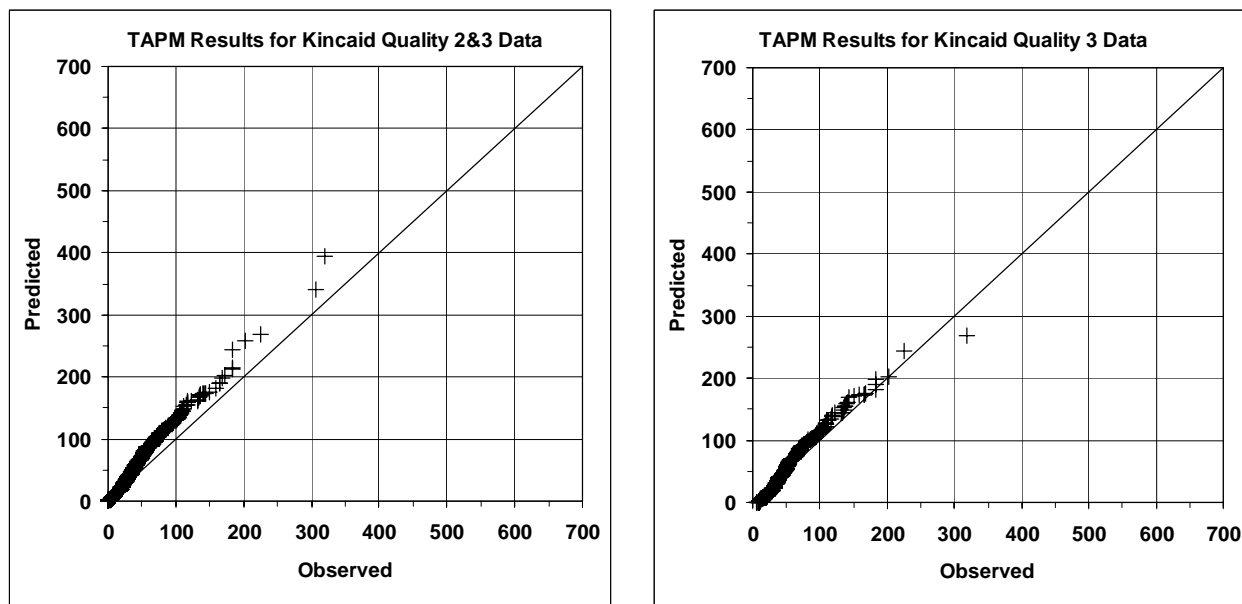


Figure 3.2. Kincaid Quantile-Quantile plots of scaled concentration for Quality 2&3 (left) and Quality 3 (right) data.

### 3.2 Indianapolis

A full description of EPRI's Indianapolis field study, conducted during 16 September to 12 October, 1985, is given in TRC (1986). It involved SF<sub>6</sub> tracer releases from the 83.8-m stack (with diameter 4.72 m) at the Perry K power plant on the southwest edge of Indianapolis, Indiana, USA (86°12'W, 39°48'N). The stack is located in a typical industrial/commercial/urban complex with many buildings within one or two kilometres (roughness length of about 1 m), and relatively flat local terrain.

Meteorological observations were taken from a 94 m height at the top of a bank building in the middle of the urban area, from two 10-m towers in suburban and rural areas, and an 11-m tower at an urban location. In addition, vertical meteorological profiles were also taken. Hourly-averaged concentrations were observed on a network of up to 160 ground-level monitors on 12 arcs at distances 0.25, 0.5, 0.75, 1.0, 1.5, 2, 3, 4, 6, 8, 10 and 12 km from the stack. To sample the plume, the network of monitors was moved so that it was downwind of the source. Data were taken in 8 or 9 hour test blocks with 19 such blocks altogether. Figure 3.3 shows the locations of the stack, meteorological sites and the tracer monitors corresponding to the test block 9. A total of 170 hours of tracer data is available, representing all stability classes and most wind speed ranges. Arc-wise maxima were calculated from the crosswind concentration variation, and a quality indicator was assigned to each value. It is recommended that only the data with quality indicator 2 (maxima identified) and 3 (maxima well defined) be used for model comparison. Out of a total of 1511 arc-hours of data, 1216 are quality 2 and 3, and 469 are quality 3.

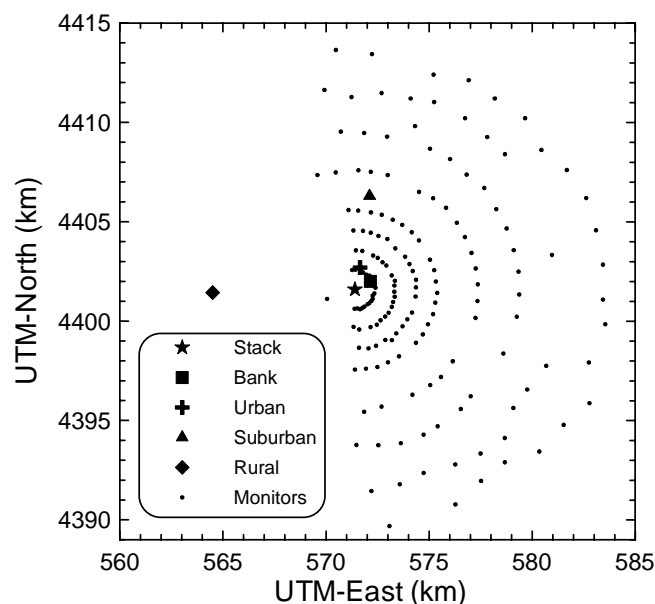


Figure 3.3. Tracer monitors (Test 9), and meteorological sites for the Indianapolis study.

TAPM V3 was run for the period 15 September to 12 October, 1985, with four nested domains of  $30 \times 30$  horizontal grid points at 30-km, 10-km, 3-km and 1-km spacing for the meteorology, and  $101 \times 101$  horizontal grid points at 7.5-km, 2.5-km, 0.75-km and 0.25-km spacing for the pollution, both centred on the stack coordinates. The 25 vertical levels were the same as in the Kincaid case. The model was run in Lagrangian mode to capture the near-source dispersion more accurately. For Indianapolis data, a value of 0.5 is recommended for

the moisture availability factor, which is defined as the ratio of the surface latent heat flux to the total surface heat flux. To match this value, we used a deep soil moisture content of  $0.3 \text{ kg kg}^{-1}$ , which was different to that used for Kincaid, as the dominant land use here was urban rather than grassland. The wind speeds and directions observed at the Urban tower (10 m AGL) and the Bank building (94 m) were assimilated into model calculations. The hourly average pollution predictions on the 0.25-km spaced grid were processed to obtain ground-level concentration maxima at the 12 arcs.

Table 3.2 lists model performance statistics for TAPM. The results show that for the Indianapolis dataset, TAPM performs well for mean and extreme performance statistics, with little bias shown by TAPM, and TAPM-NA showing some over-prediction of extreme statistics.

Figure 3.4 shows TAPM Quantile-Quantile (Q-Q) plots of the (sorted) predicted versus the (sorted) observed concentrations for both Quality 2&3 and Quality 3 data. These plots again illustrate that TAPM tends towards a very slight over-prediction for all concentration levels, except at the very low concentration end of the distribution.

Table 3.2. Model performance statistics for Indianapolis (a) for Quality 2&3 data and (b) for Quality 3 data. TAPM – with wind data assimilation. TAPM-NA – without wind data assimilation.

<b>(a) Q2&amp;3</b>	<b>MEAN</b>	<b>STD</b>	<b>NMSE</b>	<b>COR</b>	<b>IOA</b>	<b>RHC<sub>R</sub></b>	<b>MAX<sub>R</sub></b>
<b>Observed</b>	258	222	0.0	1.00	1.00	1.00	1.00
<b>TAPM</b>	251	294	1.1	0.51	0.71	1.09	1.12
<b>TAPM-NA</b>	268	356	1.5	0.46	0.64	1.36	1.46

<b>(b) Q3</b>	<b>MEAN</b>	<b>STD</b>	<b>NMSE</b>	<b>COR</b>	<b>IOA</b>	<b>RHC<sub>R</sub></b>	<b>MAX<sub>R</sub></b>
<b>Observed</b>	352	221	0.0	1.00	1.00	1.00	1.00
<b>TAPM</b>	382	328	0.7	0.46	0.66	1.14	1.21
<b>TAPM-NA</b>	414	395	1.0	0.40	0.59	1.39	1.58

Key: MEAN = Arithmetic Mean ( $\text{ng m}^{-3} (\text{g s}^{-1})^{-1}$ ), STD = Standard Deviation ( $\text{ng m}^{-3} (\text{g s}^{-1})^{-1}$ ), NMSE = normalised mean square error, COR = correlation coefficient, IOA = Index of Agreement; RHC<sub>R</sub> = Ratio (Predicted/Observed) of Robust Highest Concentration (RHC); MAX<sub>R</sub> = Ratio (Predicted/Observed) of Maximum Concentration.

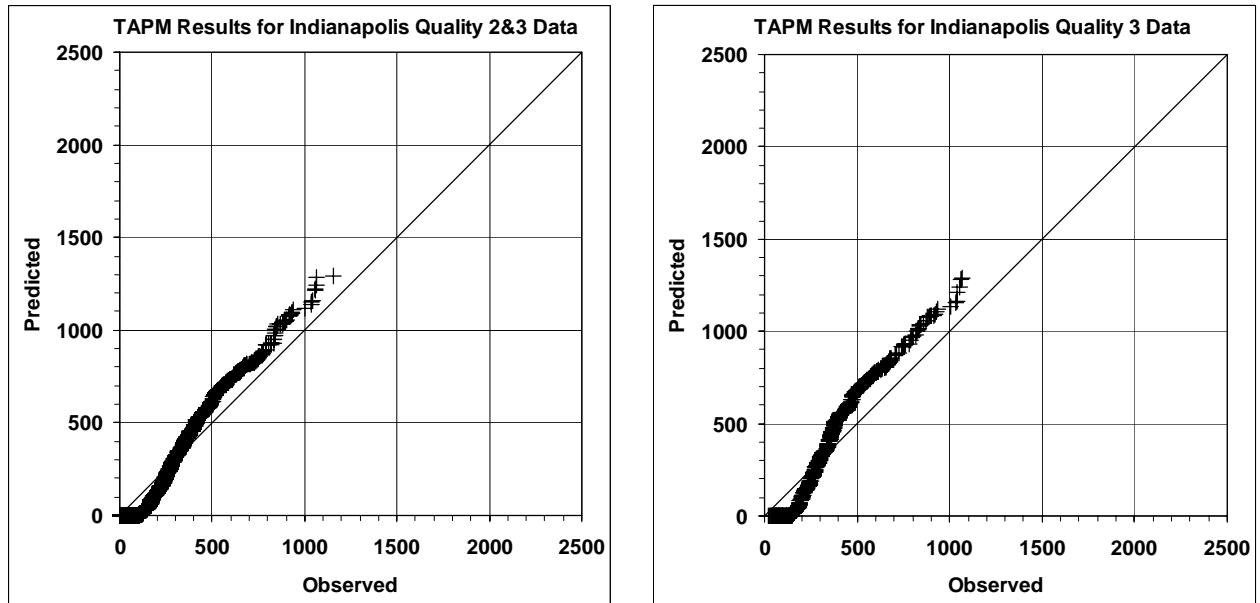


Figure 3.4. Indianapolis Quantile-Quantile plots of scaled concentration for Quality 2&3 (left) and Quality 3 (right) data.

#### 4 Anglesea

Alcoa of Australia operates a 160 MW power station within the Anglesea Heath in Victoria. This area comprises the catchment of two creeks and forms a large basin mostly surrounded by higher ground. It is well used for recreation and has high conservation value due to outstanding botanical diversity. The station has been a significant point source of sulfur emissions and a potential source of acidic deposits to the surrounding ecosystems since 1968. The power station is located at an elevation of 10 m within the naturally vegetated Anglesea River catchment (Figure 4.1). It sits, in effect, near a break in the side of a sloping 8,500 ha basin mostly surrounded by higher ground. Stack height is 110 m, which puts the point of emission roughly on a level with the edge of the basin, 3 km to the north and south. The sea is 3 km to the east.

The Anglesea region has recently been modelled for 2001 and 2002 by Hill and Hurley (2003) using TAPM V2, and for 2002 and 2003 by Hurley et al. (2005a) using TAPM V3. This Section summarises the performance of TAPM V3 from the latter study, compared to monitoring data at two sites: School – located to the south of the power station; and Mt. Ingoldsby – located south-west of the power station. Note that TAPM meteorological (wind and temperature) predictions have been verified against available observations in Hill and Hurley (2003).

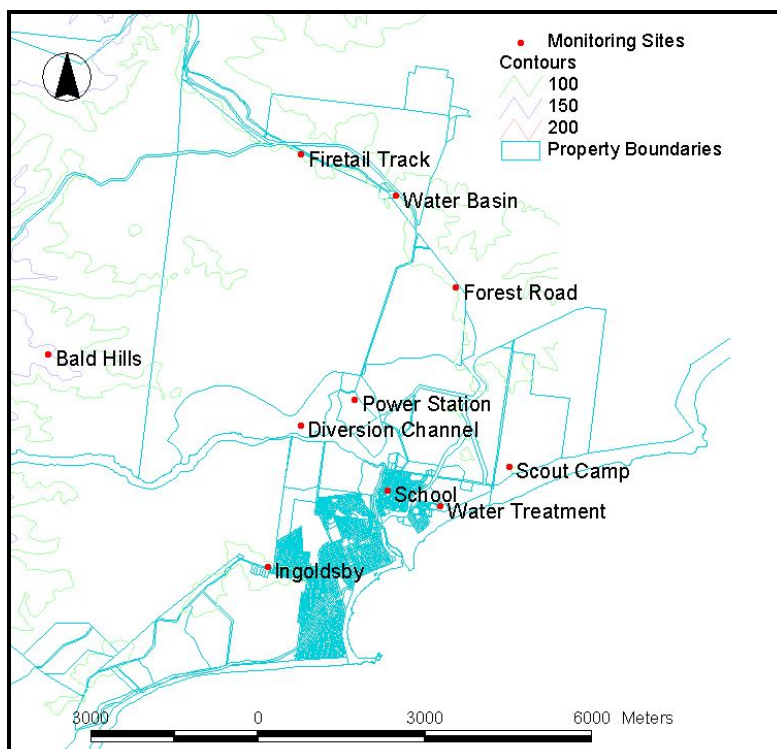


Figure 4.1. The region surrounding the Anglesea Power Station, showing terrain contours, coastline and rivers, stack location, monitoring site locations, and Anglesea township.

TAPM was used in a nested mode, centred on the power station stack, with  $25 \times 25 \times 25$  grid points and 30-km, 10-km, 3-km and 1-km spaced horizontal grids for meteorology, and with  $41 \times 41 \times 25$  grid points and 15-km, 5-km, 1.5-km and 0.5-km spaced horizontal grids for pollution. A deep-soil moisture content ranging from  $0.05 \text{ kg kg}^{-1}$  (summer) to  $0.25 \text{ kg kg}^{-1}$  (winter) was used, with default deep-soil and sea-surface temperatures. The power station stack emission characteristics input into the model included time-varying exit velocity, exit temperature and sulfur dioxide emission rate (calculated from coal use, moisture, ash and sulphur content and hourly load). The load-based emission technique used for this study has been verified to be accurate to within approximately 10% compared to in-stack emission measurements.

Figure 4.2 summarises the extreme concentrations (99.9 percentile, RHC and MAX) for each of the monitoring sites and years, and for the average (ALL) and RMSE over all sites, for observations versus TAPM. It is clear from these plots that TAPM performs well with very good average (ALL) and small RMSE for each of the statistics. TAPM over-predicts the MAX to some extent, however MAX is usually a more volatile statistic to predict.

Figure 4.3 shows Q-Q plots for the School monitoring site for 2002 and 2003 for TAPM versus the observations. This site is closer to the source than the other site, and is on the edge of the township. The plots show that TAPM does a consistently good job for both years.

Figure 4.4 shows the performance of the model when estimating maximum concentration for 5-minute-averaged concentration. The results show that the peak 5-minute averaged predictions perform as well as the predictions for the hourly-averaged results. The predicted peak-to-mean power-law exponent, averaged over the two sites for 2002 and 2003, was 0.31, compared to the average observed exponent of 0.34 – in better agreement with the data than the more commonly used generic exponent of 0.20.

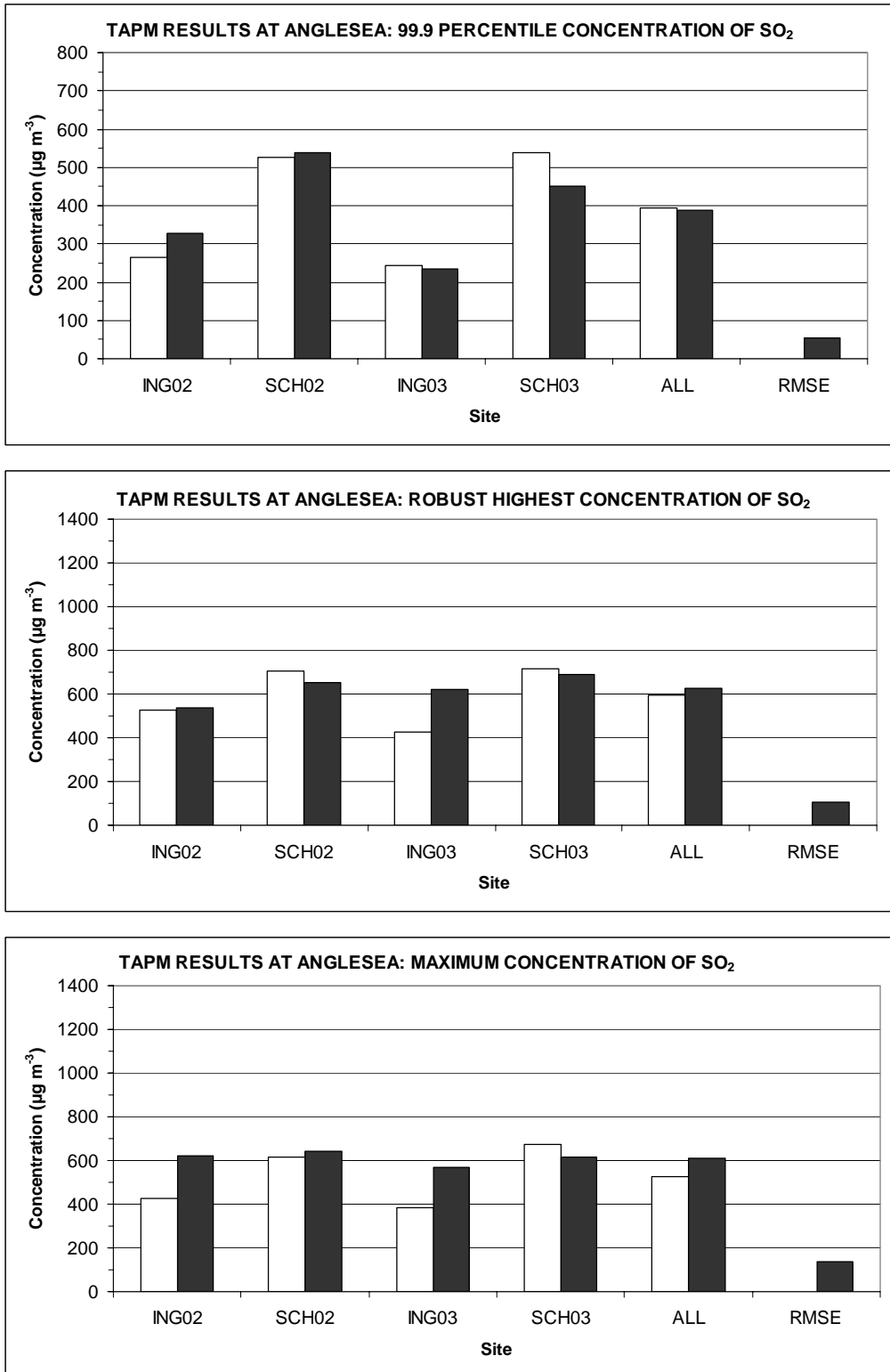


Figure 4.2: Anglesea annual extreme concentration ( $\mu\text{g m}^{-3}$ ) at the School (SCH) and Mt. Ingoldsby (ING) monitoring sites for 2002 and 2003 for the observed (OBS – white bars) concentrations and those predicted by TAPM (black bars) for 99.9 percentile (top), RHC (middle), and MAX (bottom). Note that ALL is an average over all sites and RMSE is the root mean square error over all sites.

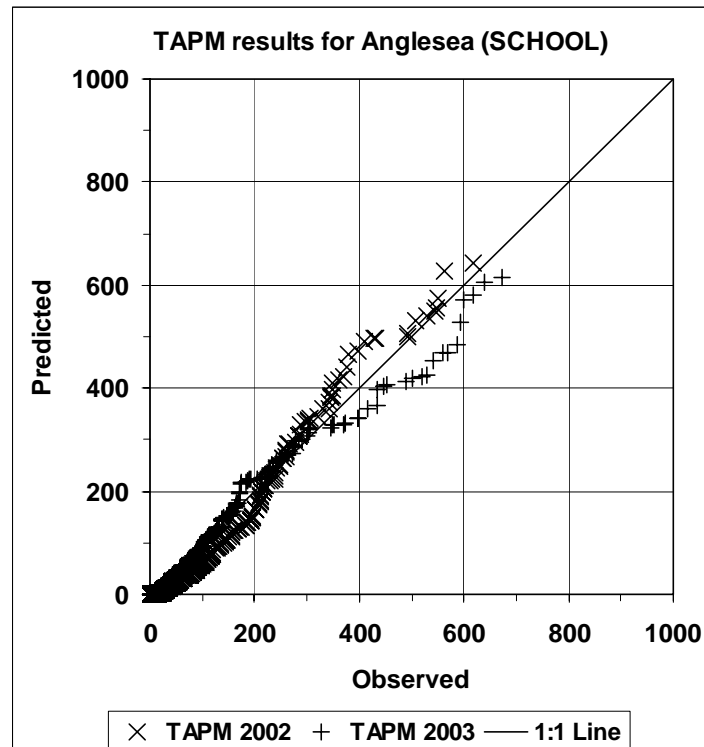


Figure 4.3: Anglesea quantile-quantile plots of the observed versus model concentration ( $\mu\text{g m}^{-3}$ ) for TAPM at the School monitoring site location for 2002 and 2003.

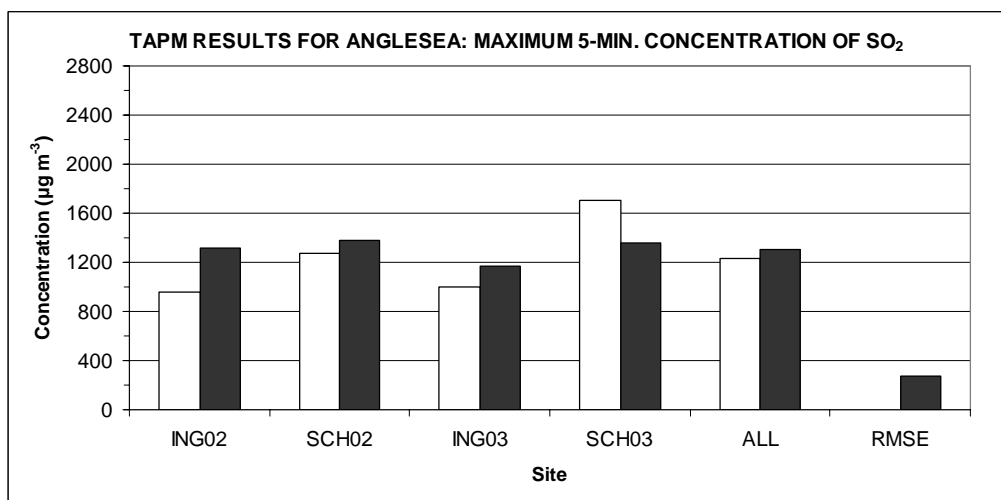


Figure 4.4: Anglesea annual maximum 5-minute averaged concentration ( $\mu\text{g m}^{-3}$ ) at the School (SCH) and Mt. Ingoldsby (ING) monitoring sites for 2002 and 2003 for the observed (OBS – white bars) concentrations and those predicted by TAPM. Note that ALL is an average over all sites and RMSE is the root mean square error over all sites.

## 5 Year-long meteorology and air pollution in the Kwinana industrial region

Kwinana ( $115^{\circ}46.5'E$ ,  $32^{\circ}11.5'S$ ) is a major heavy industrial area 30 km south of Perth, Western Australia. It is a coastal area with sea to the west (Indian Ocean) and land to the east,

an approximately north-south coastline, and relatively flat local terrain (see Figure 5.1). The Kwinana region includes industries such as power generation, refineries (oil, alumina and nickel), iron smelting, cement works, and titanium dioxide and fertilizer plants. Most of the twenty point sources are on the coast, and they have plume heights that vary from tens of metres up to a few hundred metres. The plumes generally fumigate to ground in the strong south-westerly sea-breeze flow, resulting in relatively high concentrations at distances of up to several kilometres from the coast. The regulatory framework in the region, controlled by the Department of Environmental and Water Catchment Protection (DEWCP), is a model-based control policy that uses the air quality model DISPMOD to relate ground-level concentrations back to emissions (Rayner, 1998).

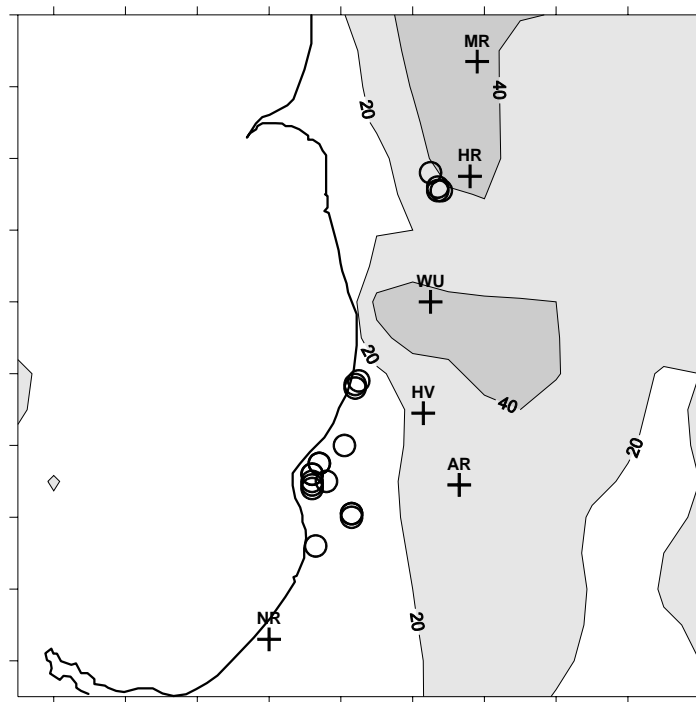


Figure 5.1. TAPM inner grid pollution domain for the Kwinana region with a west-east and south-north extent of 19 km. A detailed coastline and marked terrain height (m) contours with shading for higher heights are shown. The sources are shown as circles (O). The monitoring sites (+) correspond to: North Rockingham (NR), Abercrombie Road (AR), Hope Valley (HV), Wattleup (WU), Henderson Road (HR) and Miguel Road (MR).

The Kwinana Industries Council (KIC) was established in the course of Policy development to provide a forum for negotiations between industries and to form a single body to represent industry's viewpoint. The strong regulatory framework, and government and industry cooperation, have produced a high quality hour-by-hour emissions inventory for the industrial sources in the region. The Kwinana air monitoring network, measuring both near-surface meteorology and air pollution, was designed to capture the maximum ground level concentrations outside of the industrial zone boundaries, and near local towns, under sea-breeze fumigation conditions. The detailed emission inventory, coupled with the extensive monitoring network data, provide an excellent framework for model development and/or verification.

TAPM V3 was used to model 1997 meteorology in Kwinana (see also Hurley et al., 2005a) using nested grids of  $25 \times 25 \times 25$  points at 30-km, 10-km, 3-km and 1-km spacing for meteorology, and  $41 \times 41 \times 25$  points at 15-km, 5-km, 1.5-km and 500-m spacing for pollution. Default model options were used, except for the deep soil moisture content which varied from 0.05 (very dry) for summer months to 0.25 (moist) for winter months. Tracer mode was used for sulfur dioxide, with the four dominant point sources (of the twenty point sources in the region) run in Lagrangian (LPM) mode. More detail on the Kwinana region can be found in Hurley et al. (2001).

Model predictions were extracted at the nearest grid point to each of the six monitoring sites on the inner grid (1-km grid spacing) at the lowest model level (10 m above the ground) for winds and temperature. Sample statistics of observations and model predictions are listed in Table 5.1 for Hope Valley. The statistics used were based on the recommendations of Willmott (1981), as described in the Appendix. The results suggest that both winds and temperature are predicted well.

Table 5.1. Statistics for TAPM V3 simulation of 1997 in Kwinana (Hope Valley) for wind speed at 10 m above the ground (WS10); the west-east-component of the wind (U10); the south-north-component of the wind (V10); and temperature (T10).

VARIABLE	NUMBER	MEAN_OBS	MEAN_MOD	STD_OBS	STD_MOD	CORR	RMSE	RMSE_S	RMSE_U	IOA	SKILL_E	SKILL_V	SKILL_R
WS10	8482	4.0	4.6	1.7	1.8	0.75	1.40	0.76	1.17	0.83	0.69	1.04	0.82
U10	8482	-0.2	-0.2	3.2	3.9	0.87	1.94	0.26	1.93	0.92	0.61	1.24	0.62
V10	8482	1.1	0.6	2.8	3.0	0.84	1.70	0.53	1.61	0.91	0.58	1.09	0.62
T10	8728	18.2	18.0	5.2	6.2	0.91	2.63	0.47	2.59	0.94	0.50	1.18	0.51

KEY: OBS = Observations, MOD = Model Predictions, NUMBER = Number of hourly-averaged values used for the statistics, MEAN = Arithmetic mean, STD = Standard Deviation, CORR = Pearson Correlation Coefficient (0 = no correlation, 1 = exact correlation), RMSE = Root Mean Square Error, RMSE\_S = Systematic Root Mean Square Error, RMSE\_U = Unsystematic Root Mean Square Error, IOA = Index of Agreement (0 = no agreement, 1 = perfect agreement), SKILL\_E = (RMSE\_U)/(STD\_OBS) (<1 shows skill), SKILL\_V = (STD\_MOD)/(STD\_OBS) (near to 1 shows skill), SKILL\_R = (RMSE)/(STD\_OBS) (<1 shows skill).

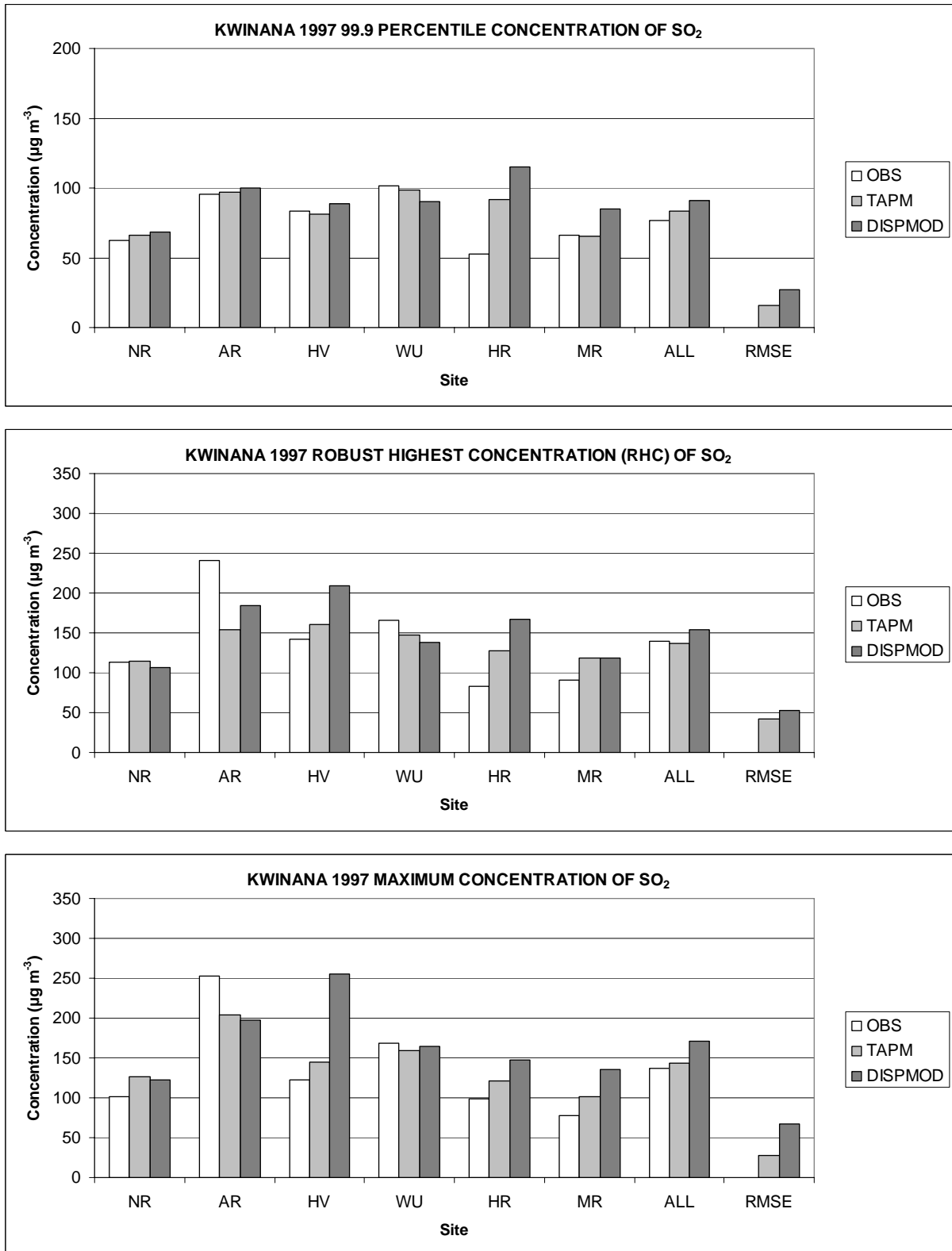


Figure 5.2: Kwinana annual extreme concentration ( $\mu\text{g m}^{-3}$ ) at all monitoring sites for 1997 for the observed (OBS) concentrations and those predicted by TAPM and DISPMOD for 99.9 percentile (top), RHC (middle), and MAX (bottom). Note that ALL is an average over all sites and RMSE is the root mean square error over all sites.

Figure 5.2 summarises the extreme concentrations (99.9 percentile, RHC and MAX) for each of the monitoring sites and years, and for the average (ALL) and RMSE over all sites, for observations versus TAPM and DISPMOD (Rayner, 1998, 2000). It is clear from these plots that TAPM performs well with very good average (ALL) and small RMSE for each of the statistics. TAPM results are slightly better overall than those of DISPMOD.

Figure 5.3 shows Q-Q plots for two monitoring sites for 1997 for TAPM versus the observations. The plots show that TAPM does a good job at both sites.

Figure 5.4 shows the performance of the model when estimating maximum concentration for 10-minute-averaged concentration, using the new concentration variance and peak-to-mean concentration options. The results show that the peak 10-minute averaged predictions perform equally as well as the predictions for the hourly-averaged results. Interestingly, the site-averaged peak-to-mean power-law exponent predicted by the new procedure was 0.27, compared to the observed exponent of 0.31 – in better agreement with the data than the more commonly used generic exponent of 0.20.

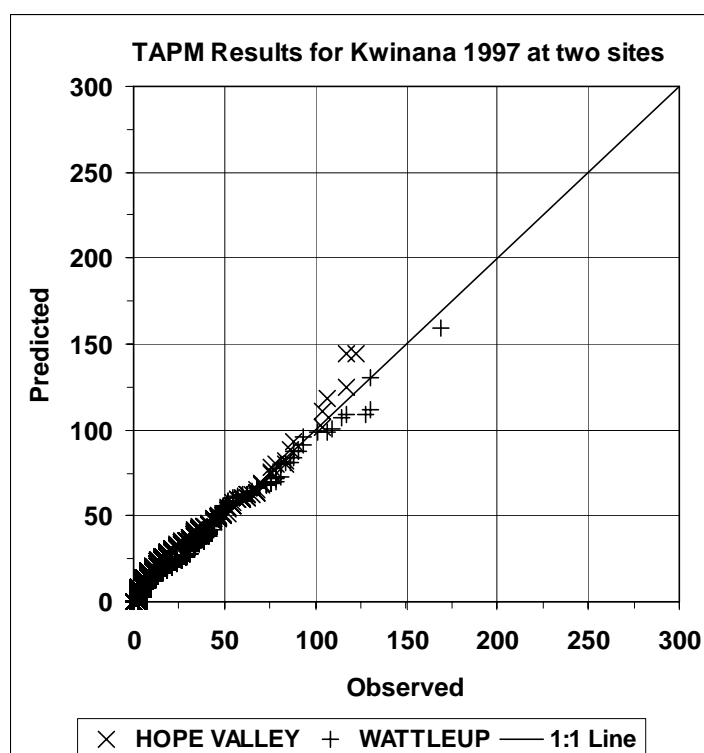


Figure 5.3: Kwinana quantile-quantile plots of the observed versus model concentration ( $\mu\text{g m}^{-3}$ ) for TAPM at two monitoring site locations for 1997.

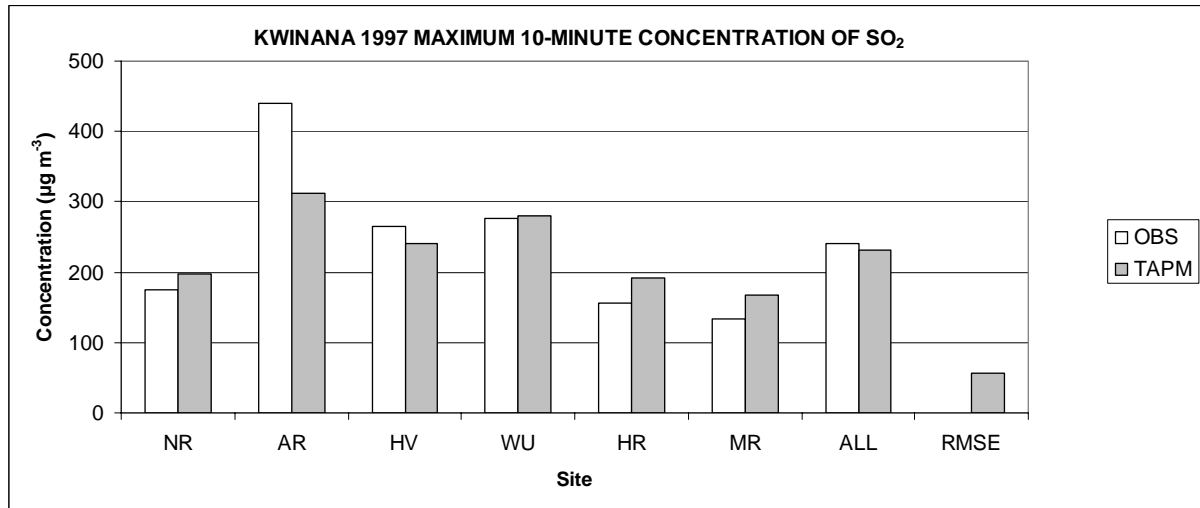


Figure 5.4: Kwinana annual maximum 10-minute averaged concentration plot at all monitoring sites for 1997 for the observed (OBS) concentrations and those predicted by TAPM. Note that ALL is an average over all sites and RMSE is the root mean square error over all sites.

## 6 Upper-Air Meteorology

### 6.1 Kalgoorlie data

The Kalgoorlie region of southern Western Australia (see Figure 6.1) is an inland industrial region with sparsely vegetated, relatively flat terrain. Western Mining Corporation (WMC) has some instrumented towers and a SODAR system (see Figure 6.1 for site locations) in the region, which are used as part of a reactive pollution control strategy to minimise the impact of industrial emissions on the local township. Edwards et al. (2004) modelled year-long meteorology in this region for 2000 using TAPM V2, and compared results with upper-level winds from a tower and a SODAR. Results were presented for annual, seasonal and diurnal statistics, as well as for a case study when a cold front passed through the region. A summary of the updated annual results for Kalgoorlie using TAPM V3 are presented here.

TAPM was used to model the meteorology of the year 2000 in the Kalgoorlie region using a nested grid of  $25 \times 25 \times 25$  points at 30-km, 10-km and 3-km horizontal grid spacing, and 25 vertical levels. A dry deep-soil moisture content of  $0.05 \text{ kg kg}^{-1}$  was used. The model predictions on the 3-km spaced grid were compared with measurements from the very closely located Kalgoorlie Nickel Smelter (KNS) tower and SODAR (see Figure 6.1 for site location).

Model predictions of hourly-averaged meteorology at model levels closest to the SODAR levels, and to the KNS tower, were extracted at the nearest grid point to each site for the 3,000-m spaced inner grid. The corresponding SODAR levels were at 50, 110, 140, 200, 260, 290, 410, 500 and 590 m, and were all within 10 m of the nearest model level. Note that the number of valid data points was reduced by about a factor of two by the 590-m height level, and by even more above this level where the data were thought to be outside the valid range of the instrument, and so were not used. Typically, this instrument is less reliable at heights above 400 m.

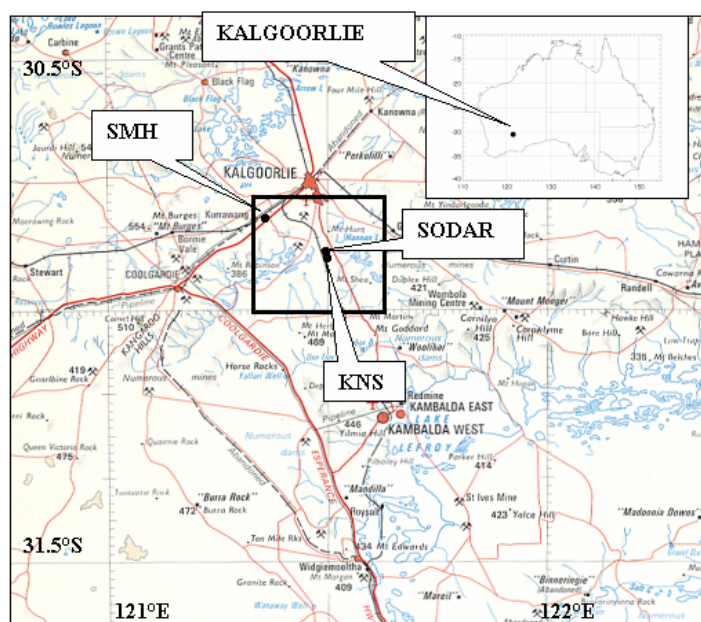


Figure 6.1. Locations of the WMC Kalgoorlie Nickel Smelter, the SMH (Seven Mile Hill) tower (not used), the KNS tower and the SODAR site. The geographical position of Kalgoorlie is also shown.

Table 6.1 shows statistics for the KNS tower for wind observed at 60 m and predicted at 50 m, temperature at 10 m, and for total solar radiation (TSR). There is some systematic bias in the results, of about  $1 \text{ m s}^{-1}$  in wind speed (due mainly to the 10 m height difference in the observations compared to predictions) and of about  $2 \text{ }^{\circ}\text{C}$  in the temperature (due to an under-prediction of night time temperature on some occasions), possibly caused by inaccurate surface parameterisation, and/or tending toward an over-prediction. Average RMSE and IOA are  $2.1 \text{ m s}^{-1}$  and 0.88 for winds,  $3.2 \text{ }^{\circ}\text{C}$  and 0.95 for temperature, and  $151 \text{ W m}^{-2}$  and 0.94 for TSR. The results indicate that the model is showing skill for each of these variables, as in all cases the standard deviations of the predicted and observed variables are within about 20%, the RMSE are much less than the observed standard deviations, and the IOA are all well above 0.5.

Tables 6.2a–c show statistics for observed (OBS) versus model predicted (MOD) winds for various model levels, compared to the SODAR data. The results show that the SODAR winds are modelled very well at all heights, and suggest that the small bias in wind speed in the tower comparisons of Table 6.1 are indeed mostly due to the 10-m height difference that is more critical for heights near the ground. The mean and standard deviations are all within  $0.5 \text{ m s}^{-1}$  for all heights, the RMSE increases from about  $1.5 \text{ m s}^{-1}$  for the 50-m level to about  $3.0 \text{ m s}^{-1}$  at the 600-m level for wind speed (slightly higher for the wind components), and the average IOA are 0.87 for wind speed, 0.96 for the west-east ( $u$ ) component and 0.93 for the south-north ( $v$ ) component (an average of 0.92 for winds). The level of skill shown at all levels indicates that the standard deviations of the predicted and observed variables are within about 10%, the RMSE are much less than the observed standard deviations, and the IOA are all well above 0.5 – in fact they are all 0.84 or higher.

In summary, the results show that TAPM is able to capture well the meteorology of the region. Seasonal and diurnal variation of winds (not shown here) were also predicted well, with no bias shown towards better performance at particular times of the year or day.

Table 6.1. Wind ( $w_s$ ,  $u$  and  $v$ ), temperature at 10 m (T10) and Total Solar Radiation (TSR) statistics for TAPM simulation of 2000 at the KNS tower site (Note that the tower wind data are from a height of 60 m, while the model wind data are from 50 m).

	NUMBER	MEAN_OBS	MEAN_MOD	STD_OBS	STD_MOD	CORR	RMSE	RMSE_S	RMSE_U	IOA	SKILL_E	SKILL_V	SKILL_R
<b>WS60</b>	8584	6.3	5.2	2.3	1.9	0.70	2.05	1.54	1.34	0.77	0.57	0.80	0.87
<b>U60</b>	8584	-1.2	-0.8	5.1	4.3	0.91	2.14	1.22	1.75	0.95	0.35	0.85	0.42
<b>V60</b>	8584	0.6	0.4	4.3	3.4	0.86	2.19	1.38	1.70	0.91	0.40	0.79	0.51
<b>T10</b>	8580	19.5	17.7	6.4	7.2	0.93	3.17	1.83	2.59	0.95	0.40	1.13	0.49
<b>TSR</b>	8584	202	249	286	348	0.92	151	58	140	0.94	0.49	1.22	0.53

KEY: OBS = Observations, MOD = Model Predictions, MEAN = Arithmetic mean, STD = Standard Deviation, CORR = Pearson Correlation Coefficient (0=no correlation,1=exact correlation), RMSE = Root Mean Square Error, RMSE\_S = Systematic Root Mean Square Error, RMSE\_U = Unsystematic Root Mean Square Error, IOA = Index of Agreement (0=no agreement, 1=perfect agreement), SKILL\_E = (RMSE\_U)/(STD\_OBS) (<1 shows skill), SKILL\_V = (STD\_MOD)/(STD\_OBS) (near to 1 shows skill), SKILL\_R = (RMSE)/(STD\_OBS) (<1 shows skill).

Table 6.2a. Wind speed ( $m s^{-1}$ ) statistics for TAPM simulation of 2000 at the SODAR site.

HEIGHT	NUMBER	MEAN_OBS	MEAN_MOD	STD_OBS	STD_MOD	CORR	RMSE	RMSE_S	RMSE_U	IOA	SKILL_E	SKILL_V	SKILL_R
<b>50 m</b>	7846	5.6	5.2	2.1	1.9	0.73	1.55	0.84	1.30	0.84	0.62	0.90	0.74
<b>100 m</b>	7851	6.7	6.4	2.6	2.3	0.74	1.82	0.94	1.56	0.85	0.60	0.89	0.70
<b>150 m</b>	7713	7.1	7.3	2.9	2.8	0.76	1.97	0.78	1.81	0.87	0.63	0.97	0.69
<b>200 m</b>	7263	7.8	8.0	3.3	3.2	0.77	2.24	0.85	2.07	0.87	0.63	0.99	0.68
<b>250 m</b>	6762	8.3	8.5	3.7	3.6	0.79	2.36	0.81	2.21	0.89	0.60	0.99	0.64
<b>300 m</b>	6486	8.5	8.9	3.8	4.0	0.80	2.51	0.78	2.38	0.89	0.62	1.03	0.65
<b>400 m</b>	5514	9.1	9.3	4.2	4.4	0.80	2.73	0.76	2.63	0.89	0.62	1.03	0.65
<b>500 m</b>	4935	9.6	9.6	4.4	4.6	0.80	2.84	0.78	2.73	0.89	0.62	1.03	0.64
<b>600 m</b>	4483	10.2	9.7	4.6	4.7	0.79	3.00	1.00	2.83	0.89	0.62	1.02	0.66

KEY: Same as for Table 6.1.

Table 6.2b. West-east ( $u$ ) component of the wind ( $m s^{-1}$ ) statistics for TAPM simulation of 2000 at the SODAR site.

	NUMBER	MEAN_OBS	MEAN_MOD	STD_OBS	STD_MOD	CORR	RMSE	RMSE_S	RMSE_U	IOA	SKILL_E	SKILL_V	SKILL_R
<b>50 m</b>	7846	-1.1	-0.8	4.6	4.3	0.92	1.78	0.73	1.63	0.96	0.35	0.93	0.39
<b>100 m</b>	7851	-1.3	-1.1	5.5	5.2	0.92	2.11	0.67	2.00	0.96	0.37	0.96	0.39
<b>150 m</b>	7713	-1.4	-1.3	5.8	6.0	0.93	2.29	0.28	2.27	0.96	0.39	1.03	0.39
<b>200 m</b>	7263	-1.1	-1.5	6.4	6.7	0.93	2.50	0.41	2.46	0.96	0.39	1.05	0.39
<b>250 m</b>	6762	-1.5	-1.6	6.9	7.1	0.93	2.60	0.26	2.59	0.96	0.38	1.04	0.38
<b>300 m</b>	6486	-1.5	-1.7	7.1	7.5	0.93	2.70	0.18	2.69	0.97	0.38	1.06	0.38
<b>400 m</b>	5514	-1.5	-1.6	7.8	8.1	0.93	2.91	0.27	2.90	0.97	0.37	1.04	0.37
<b>500 m</b>	4935	-1.4	-1.4	8.3	8.4	0.94	3.01	0.40	2.98	0.97	0.36	1.02	0.36
<b>600 m</b>	4483	-1.2	-1.1	8.8	8.6	0.93	3.15	0.74	3.06	0.97	0.35	0.98	0.36

KEY: Same as for Table 6.1.

Table 6.2c. South-north (*v*) component of the wind ( $\text{m s}^{-1}$ ) statistics for TAPM simulation of 2000 at the SODAR site.

HEIGHT	NUMBER	MEAN_OBS	MEAN_MOD	STD_OBS	STD_MOD	CORR	RMSE	RMSE_S	RMSE_U	IOA	SKILL_E	SKILL_V	SKILL_R
<b>50 m</b>	7846	0.6	0.4	3.6	3.4	0.86	1.88	0.78	1.71	0.93	0.47	0.93	0.51
<b>100 m</b>	7851	0.7	0.3	4.4	4.2	0.87	2.29	0.89	2.11	0.93	0.48	0.95	0.52
<b>150 m</b>	7713	0.7	0.2	4.8	4.8	0.87	2.52	0.77	2.40	0.93	0.50	1.01	0.53
<b>200 m</b>	7263	0.9	0.1	5.3	5.4	0.88	2.77	1.00	2.59	0.93	0.48	1.00	0.52
<b>250 m</b>	6762	0.5	0.0	5.8	5.7	0.89	2.75	0.86	2.61	0.94	0.45	0.99	0.48
<b>300 m</b>	6486	0.5	-0.1	5.9	5.9	0.89	2.80	0.82	2.68	0.94	0.46	1.01	0.48
<b>400 m</b>	5514	0.6	0.0	6.2	6.1	0.89	2.92	0.94	2.77	0.94	0.45	0.99	0.47
<b>500 m</b>	4935	0.7	-0.1	6.5	6.3	0.89	3.07	1.17	2.83	0.94	0.44	0.97	0.47
<b>600 m</b>	4483	0.7	-0.2	6.7	6.3	0.88	3.31	1.45	2.98	0.93	0.45	0.94	0.50

KEY: Same as for Table 6.1.

## 6.2 Pilbara data

For the Burrup Peninsula region of Western Australia, TAPM V2 simulations have been carried out for winter (July 1998) and summer (January 1999) months, as well as the seasonal transition months (April 1998 and October 1998) (Physick et al., 2004). The model results were compared to observed surface and upper-air winds (half-hourly averaged acoustic radar data) at DEPWA's Karratha site. Monthly-mean winds were used in the analysis as a method for evaluating the model's ability to simulate the variation of the wind patterns with height and season. Monthly TAPM V2 simulations have also been carried out for the Port Hedland region, 200 km east of Karratha in Western Australia (Physick et al., 2004), and results

compared to twice daily radiosonde data. Based on the similarity between results for TAPM V2 and V3 for Kalgoorlie, we expect TAPM V3 results will be similar to the good results presented using TAPM V2 for the Pilbara studies. In Section 7, TAPM V3 results will be presented for near-surface meteorology as well as for dispersion in the Pilbara region.

## **7 Meteorology and air pollution in the Pilbara**

The Pilbara region of Western Australia occupies a large part of the sparsely-populated north-west of the state. The coastal towns of Dampier and Karratha, 1500 km north of Perth, service local industry (established on the Burrup Peninsula as a result of offshore natural gas) and the ore-loading facilities set up to ship ore transported by rail from inland mining areas. Figure 7.1 shows a map of the area with monitoring sites and significant emitters of pollutants.

Woodside is the operator of the North West Shelf Venture (NWSV), which is Australia's largest resource development project. The existing Onshore Gas Plant (OGP) is located at Withnell Bay, near Dampier on the Burrup Peninsula. Production of domestic gas commenced in 1984 with gas and liquids supplied from the North Rankin A platform. Liquefied Natural Gas (LNG) production commenced in 1989 with the completion of LNG Trains 1 and 2. The third LNG train was completed in 1993. Liquefied Petroleum Gas (LPG) storage and ship loading facilities were completed in 1995 to coincide with the commencement of production from the Goodwyn Alpha platform. Also in 1995 the FPSO Cossack Pioneer commenced to supply gas to the OGP. In February 2000 Woodside received environmental approval for an additional two LNG Trains.

Meteorological and air quality data were collected in the Pilbara region from early 1998 until the end of 2001. An analysis of these data sets established that low-level coastal winds in the Burrup Peninsula region were predominantly north-easterly to south-easterly from April to August, and north-westerly to south-westerly from September to March. However in those transition months between summer and winter there were many days when the wind direction in the lowest 800 m rotated through 360° over a 24-hour period, often for several consecutive days. It was surmised that the wind behaviour on such days might lead to the recirculation of coastal emissions. Coastal fumigation was also identified as an important process for the dispersion of plumes from elevated sources. In a follow-up study to evaluate the performance of three air quality models in the region, it was found that TAPM was able to simulate the above processes. See Physick et al. (2004) for more detail on these studies.

In this Section, we present an updated summary of the air quality verification study in the Burrup Peninsula region using TAPM V3. See Hurley et al. (2003b) for the TAPM V2 verification study.

TAPM was used in a nested mode with  $25 \times 25 \times 25$  grid points and 30-km, 10-km, 3-km, 1-km and 0.5-km spaced horizontal grids for meteorology, and with  $41 \times 41 \times 25$  grid points and 15-km, 5-km, 1.5-km, 0.5-km and 0.25-km spaced horizontal grids for pollution. Note that the area covered by each pollution grid is slightly less than the area of the corresponding meteorological grid. In this way, the pollution grids avoid the boundary regions of the nested meteorological grids, where spurious vertical velocities can sometimes occur. The lowest ten model levels were at heights of 10, 25, 50, 100, 150, 200, 250, 300, 400 and 500 m, with the model top at 8 km. TAPM was configured for the Burrup Peninsula using the default databases of terrain and land use, except for some modifications around the Burrup Peninsula that account for:

- some inaccuracies in these fields due to the coarseness (approximately 1-km grid spacing) of the default land use and land/sea mask;
- the regional salt ponds;
- the roughness of the sub-grid scale terrain not resolved by the model.

The synoptic analyses used to drive the model were the LAPS analyses (for a description of LAPS see Puri et al., 1998) for the modelled year 1999. For each month, a deep soil moisture content of  $0.1 \text{ kg kg}^{-1}$  was used, with default deep-soil and sea-surface temperatures.

Background concentrations for  $\text{O}_3$  (25 ppb) and Rsmog (0.2 ppb), were based on the earlier studies. Emissions from fires have also been ignored, and days of smoky air were removed (due to enhanced  $\text{O}_3$  levels) from the Dampier and King Bay pollution monitoring data used for model comparisons.

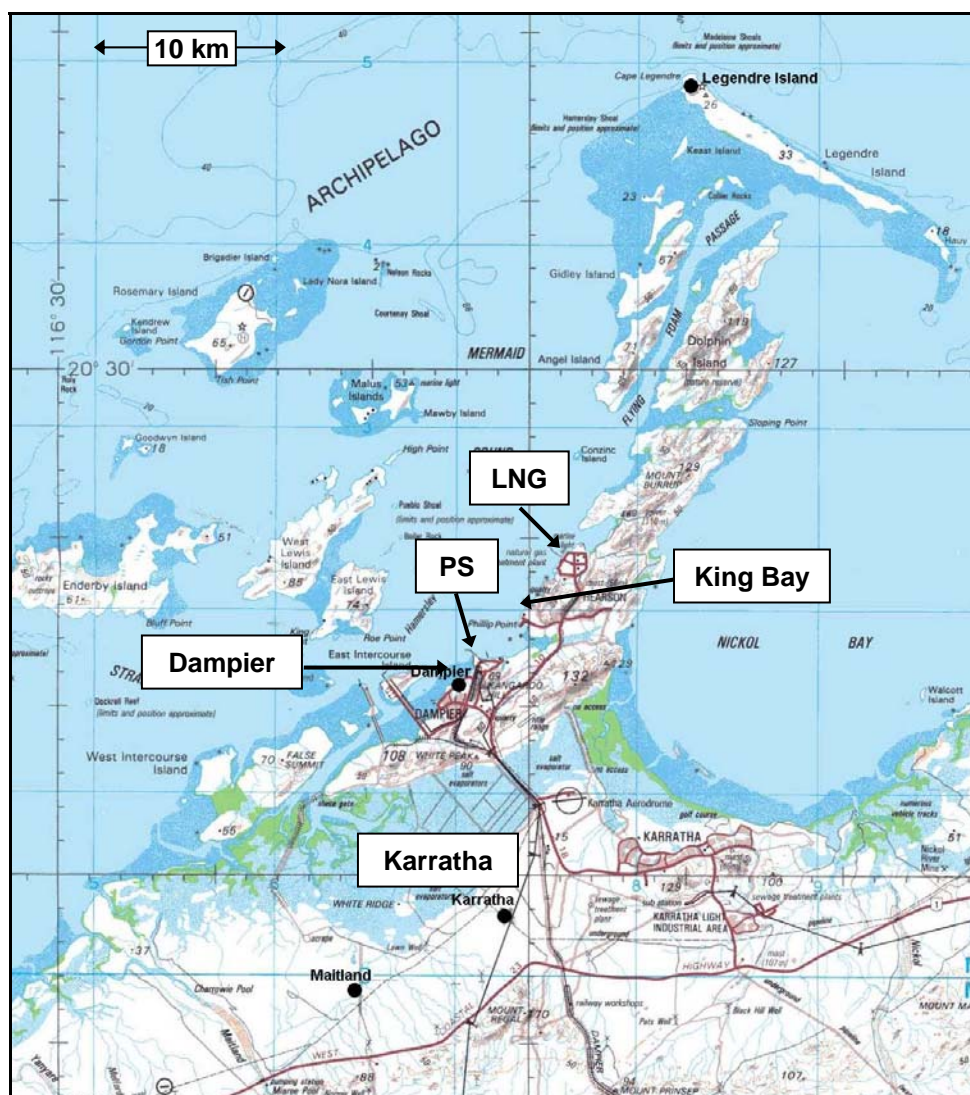


Figure 7.1. The Burrup Peninsula region, including the data sites, King Bay, Dampier and Karratha, and the emission point sources East Intercourse Dampier power station (PS) and the liquefied natural gas (LNG) plant.

The gridded emission inventory used for modelling consisted of biogenic emissions, and surface emissions representing towns, roads, ships, wharfs and other area sources. Woodside

provided point source emissions for Hamersley Iron’s Dampier power station and Woodside’s OGP. Buoyancy enhancement factors (EF) were calculated for LNG Plant sources using the stack locations provided by Woodside, with a representative (conservative) plume rise of 150 m, based on TAPM plume-rise calculations for these sources using no buoyancy enhancement. More detail on emissions is contained in Hurley et al. (2003b).

TAPM was run for the year 1999 and results were assessed against observations from available monitoring sites for meteorology (Dampier and Karratha) and pollution (Dampier and King Bay) using standard performance measures – see the Appendix for details.

Annual statistics for wind speed, east-west and north-south components of the wind, temperature and relative humidity, all at a height of 10 m above the ground, have been extracted for the TAPM simulation on the finest grid available for each site and are presented in Table 7.1 for Dampier and Karratha. At both sites, statistics are very good as the indexes of agreement are especially high, thus indicating that the model is showing excellent skill. Note that the predicted wind speed at Dampier is higher than observed, but this is due to the fact that Dampier wind observations are affected by very local effects (trees), thus reducing the observed wind speeds. These good results give confidence in the use of TAPM meteorology to drive the pollution predictions for this region.

Table 7.1. Annual statistics at Dampier and Karratha for TAPM simulation of 1999 for the following surface variables (10 m above the ground): wind speed (WS) ( $\text{m s}^{-1}$ ), the west-east component of the wind (U) ( $\text{m s}^{-1}$ ), the south-north component of the wind (V) ( $\text{m s}^{-1}$ ), temperature (T) ( $^{\circ}\text{C}$ ), and relative humidity (RH) (%).

VARIABLE	NUMBER	MEAN_OBS	MEAN_MOD	STD_OBS	STD_MOD	CORR	RMSE	RMSE_S	RMSE_U	IOA	SKILL_E	SKILL_V	SKILL_R
<b>DAMPIER</b>													
WS	8405	3.8	4.3	1.7	1.7	0.42	1.94	1.14	1.57	0.65	0.90	0.99	1.11
U	8405	0.3	-0.6	3.3	3.7	0.83	2.26	0.95	2.05	0.89	0.62	1.12	0.68
V	8405	0.0	0.2	2.5	2.7	0.74	1.91	0.55	1.83	0.85	0.72	1.08	0.76
T	8668	25.8	25.4	3.9	4.3	0.90	1.96	0.37	1.93	0.94	0.50	1.13	0.51
RH	8633	60.9	60.4	18.2	18.3	0.76	12.73	4.30	11.98	0.87	0.66	1.01	0.70
<b>KARRATHA</b>													
WS	8736	4.4	4.2	2.3	1.7	0.66	1.77	1.23	1.27	0.78	0.55	0.73	0.76
U	8736	0.2	-0.4	4.1	3.4	0.86	2.17	1.35	1.69	0.91	0.41	0.81	0.52
V	8736	-0.3	0.1	2.8	3.0	0.78	1.99	0.59	1.90	0.87	0.67	1.06	0.70
T	8737	25.6	25.0	5.0	6.3	0.91	2.73	0.92	2.57	0.94	0.51	1.25	0.54
RH	8736	60.3	56.1	21.9	21.5	0.79	14.57	6.43	13.07	0.88	0.60	0.98	0.66

KEY: OBS = Observations, MOD = Model Predictions, NUMBER = Number of hourly-averaged values used for the statistics, MEAN = Arithmetic mean, STD = Standard Deviation, CORR = Pearson Correlation Coefficient (0 = no correlation, 1 = exact correlation), RMSE = Root Mean Square Error, RMSE\_S = Systematic Root Mean Square Error, RMSE\_U = Unsystematic Root Mean Square Error, IOA = Index of Agreement (0 = no agreement, 1 = perfect agreement), SKILL\_E =  $(\text{RMSE}_U)/(\text{STD}_{\text{OBS}})$  (<1 shows skill), SKILL\_V =  $(\text{STD}_{\text{MOD}})/(\text{STD}_{\text{OBS}})$  (near to 1 shows skill), SKILL\_R =  $(\text{RMSE})/(\text{STD}_{\text{OBS}})$  (<1 shows skill).

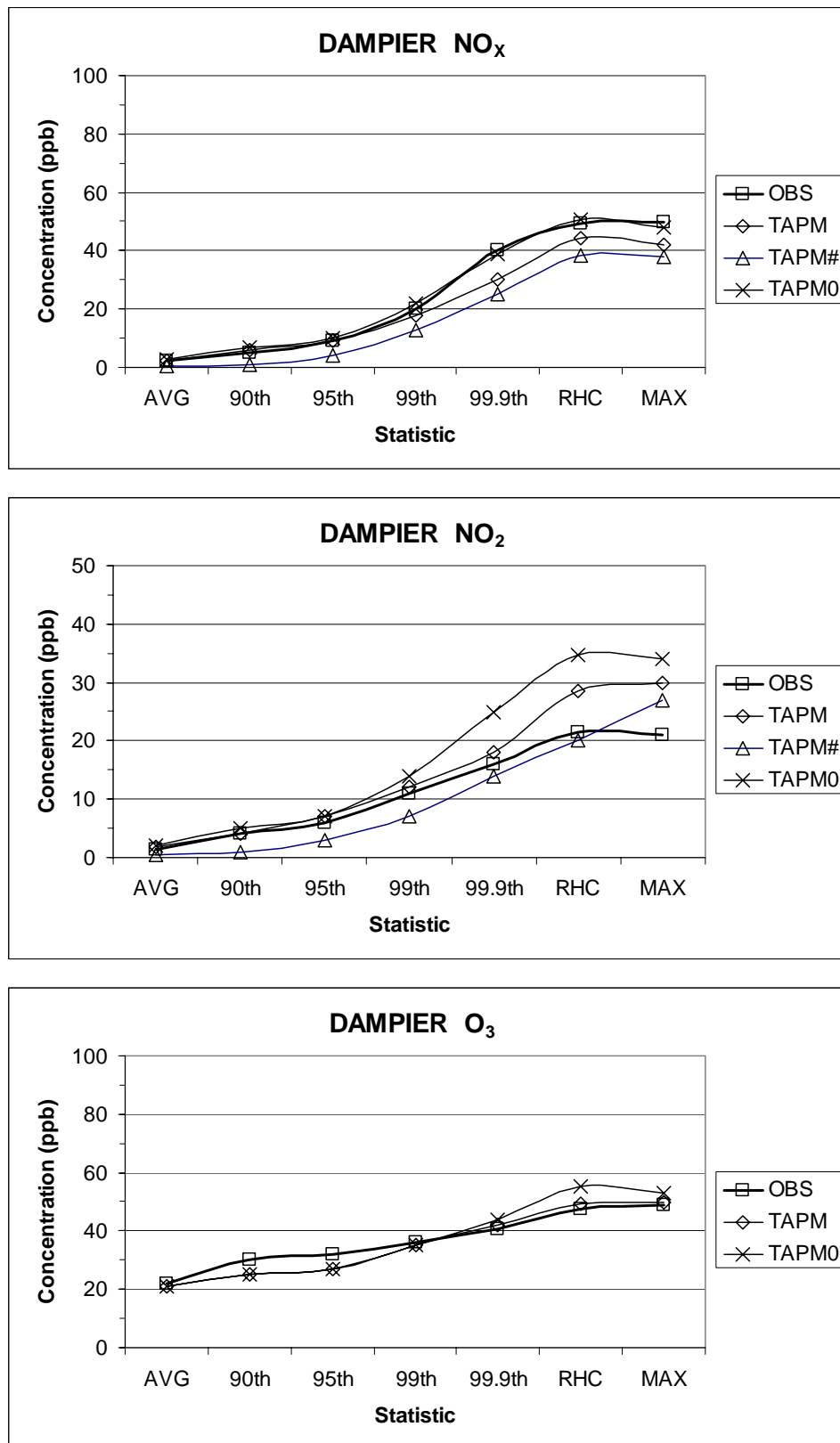


Figure 7.2. Annual statistics (Dampier 1999 – average (AVG), percentiles, Robust Highest Concentration (RHC), and the maximum (MAX)) for NO<sub>x</sub>, NO<sub>2</sub> and O<sub>3</sub>. Note that TAPM# excludes area source and biogenic emissions and TAPM0 excludes buoyancy enhancement.

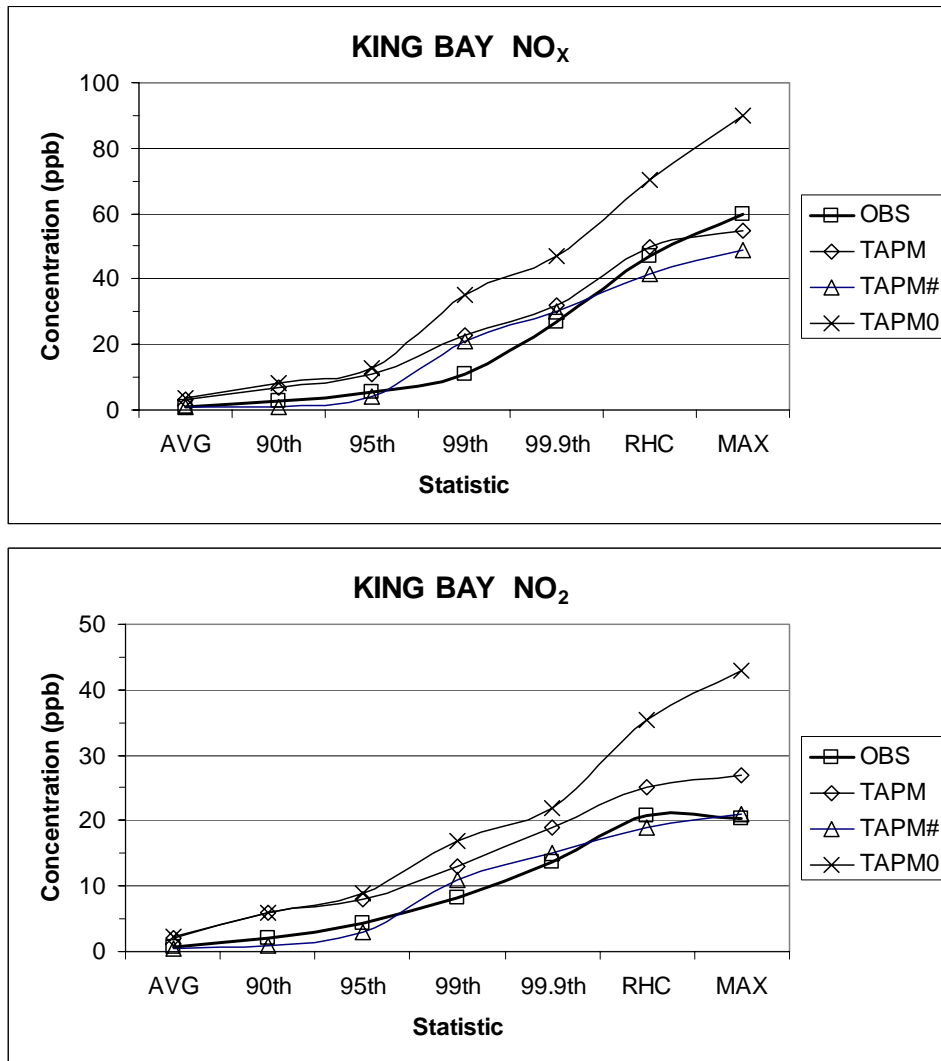


Figure 7.3. Annual statistics (King Bay 1999 – average (AVG), percentiles, Robust Highest Concentration (RHC), and the maximum (MAX)) for NO<sub>x</sub> and NO<sub>2</sub>. Note that TAPM# excludes area source and biogenic emissions and TAPM0 excludes buoyancy enhancement.

Annual statistics (average (AVG), percentiles, Robust Highest Concentration (RHC), and the maximum (MAX)) for NO<sub>x</sub>, NO<sub>2</sub> and O<sub>3</sub> at the Dampier and King Bay monitoring sites, are plotted in Figures 7.2 and 7.3 (denoted as TAPM in the Figures). Two sets of sensitivity results are also shown in the Figures, for simulations that exclude either:

- gridded area sources and biogenics (TAPM#),
- or buoyancy enhancement (TAPM0).

The results at Dampier show that NO<sub>x</sub> and NO<sub>2</sub> are predicted well, with good prediction of the average and extreme concentrations, although some minor underestimation of the extreme NO<sub>x</sub> and minor overestimation of the extreme NO<sub>2</sub> has occurred. When gridded area sources are removed, the NO<sub>x</sub> and NO<sub>2</sub> concentrations at Dampier are lower, and the extreme concentrations (RHC and MAX) for NO<sub>2</sub> are a little closer to the observations, although there is only a minor difference in the 99.9<sup>th</sup> percentile (approximately the 9<sup>th</sup> highest concentration).

The results at King Bay show that  $\text{NO}_x$  and  $\text{NO}_2$  are predicted well, although there is a general overestimation of the average and lower percentiles of  $\text{NO}_x$ , and a general overestimation of  $\text{NO}_2$  for all concentration levels. When gridded area sources are removed, the concentrations at King Bay decrease, particularly the average and lower percentiles, and the overall comparisons are very close to the observations. This indicates that the King Bay wharf emissions seem to be too high. However this emission overestimation will only really affect the average and lower percentiles of the concentration distribution in the King Bay region, with minimal impact on the extreme and/or regional maximum concentrations. When buoyancy enhancement of the LNG plumes is not used, the result is a significant increase in the extreme  $\text{NO}_x$  and  $\text{NO}_2$  concentrations, showing results at King Bay are sensitive to this effect, unlike at Dampier. This is likely to be due to King Bay being much closer to the LNG Plant than Dampier.

## 8 Annual urban meteorology and air pollution in Melbourne

Melbourne (144°53'E, 37°49'S) is a coastal city in the southern part of Victoria, Australia, with ocean to the south and mountains to the north. The EPA Victoria operates an air monitoring network covering the urban region of Melbourne, and measures both near-surface meteorology and air pollution (see Figure 8.1). This Section summarises the results from TAPM modelling of year-long (July 1997 to June 1998) meteorology and photochemical air pollution in Melbourne (Hurley *et al.*, 2003a), which was an update/extension of the verification component of the work performed as part of the EPA Victoria Air Quality Improvement Plan.

TAPM was configured with three (nested) grids of  $25 \times 25 \times 25$  points at 30-km, 10-km and 3-km spacing for meteorology, and  $41 \times 41 \times 25$  points at 15-km, 5-km and 1.5-km spacing for pollution. Default model options were used, except that deep soil moisture content varied linearly from 0.05 (very dry) for summer months to 0.25 (moist) for winter months. Land-use was dominated by urban characteristics for most of the nine Melbourne monitoring sites.

The emissions inventory covered Melbourne and Geelong, as well as major point sources in the Latrobe Valley about 100 km east of Melbourne. It represents emissions for all pollutants on approximately a 1-km spaced grid for vehicle, commercial and domestic emissions, as well as a point-source inventory, and a biogenic-emission inventory on a 3-km spaced grid (nitrogen oxides and hydrocarbons only). The emission inventory was developed for the Melbourne region by EPA Victoria for both general EPA use, and for use by the Australian Air Quality Forecasting System (AAQFS). Non-zero background concentrations were used for ozone (15 ppb), smog reactivity ( $R_{\text{smog}} = 0.7$  ppb) and particles ( $10 \mu\text{g m}^{-3}$  for  $\text{PM}_{10}$  and  $5 \mu\text{g m}^{-3}$  for  $\text{PM}_{2.5}$ , to account for dust and sea salt emissions not in the inventory), and the standard reactivity coefficient for  $R_{\text{smog}}$  of 0.0067 was used for all VOC emissions.

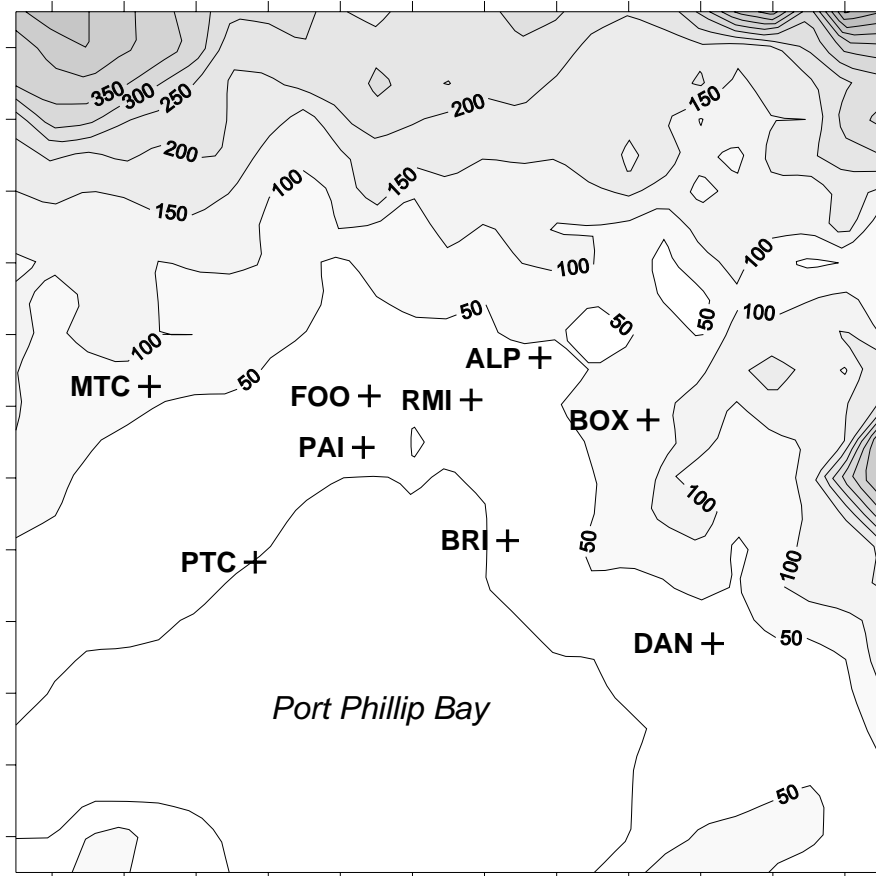


Figure 8.1. TAPM inner grid domain for Melbourne at 3000-m resolution with a west-east and south-north extent of 72 km. Terrain height (m) contours with shading for higher heights are shown. The EPAV monitoring sites are marked, and correspond to: Alphington (ALP), Box Hill (BOX), Brighton (BRI), Dandenong (DAN), Footscray (FOO), Mt. Cottrell (MTC), Paisley (PAI), Pt. Cook (PTC) and RMIT (RMI).

Table 8.1. Statistics for TAPM simulation without meteorological data assimilation of July 1996 – June 1997 in Melbourne (averaged over eight sites) for wind speed at 10 m above the ground (WS); the west-east-component of the wind (U); the south-north-component of the wind (V); and screen-level temperature (T).

VARIABLE	NUMBER	MEAN_OBS	MEAN_MOD	STD_OBS	STD_MOD	CORR	RMSE	RMSE_S	RMSE_U	IOA	SKILL_E	SKILL_V	SKILL_R
WS	8295	3.3	3.3	1.9	1.7	0.74	1.36	0.70	1.15	0.84	0.63	0.93	0.73
U	8295	0.8	1.0	2.1	2.1	0.76	1.45	0.55	1.33	0.87	0.66	1.02	0.71
V	8295	0.3	0.0	3.0	2.9	0.86	1.62	0.59	1.50	0.92	0.51	0.99	0.55
T	8621	14.6	14.5	5.9	6.7	0.93	2.66	0.71	2.54	0.95	0.43	1.13	0.45

KEY: OBS = Observations, MOD = Model Predictions, NUMBER = Number of hourly-averaged values used for the statistics, MEAN = Arithmetic mean, STD = Standard Deviation, CORR = Pearson Correlation Coefficient (0 = no correlation, 1 = exact correlation), RMSE = Root Mean Square Error, RMSE\_S = Systematic Root Mean Square Error, RMSE\_U = Unsystematic Root Mean Square Error, IOA = Index of Agreement (0 = no agreement, 1 = perfect agreement), SKILL\_E = (RMSE\_U)/(STD\_OBS) (<1 shows skill), SKILL\_V = (STD\_MOD)/(STD\_OBS) (near to 1 shows skill), SKILL\_R = (RMSE)/(STD\_OBS) (<1 shows skill).

In order to examine the sensitivity of pollution results to predicted winds when simulating urban air pollution, the model was run twice in Hurley et al. (2003a). The first run was in normal mode without meteorological data assimilation, and the second run was in data assimilation mode using Melbourne and Geelong monitoring site 10-m level wind speed and direction data. The second run used data assimilation site characteristics with a 20-km radius of influence, and assimilated the observed winds for the lowest two model levels (10 m and 25 m). The results showed that the inclusion of wind data assimilation for Melbourne did not improve annual statistics of pollution (e.g. mean, 99.9 percentile, robust highest concentration or maximum concentration). The results summarised below are for TAPM V3 without wind data assimilation.

Model predictions of meteorology were extracted at the nearest grid point to each of the eight meteorological monitoring sites on the inner grid (3-km spacing) at 10 m above the ground for winds and at screen-level for temperature. Statistics of observations and model predictions are shown in Table 8.1, and are based on the recommendations of Willmott (1981) – see the Appendix for details. The results suggest that both winds and temperature are predicted very well, with no significant biases, low RMSE and high IOA. The average RMSE and IOA for winds are  $1.5 \text{ m s}^{-1}$  and 0.88, and for temperature are 2.7 C and 0.95, which are very good results.

Ground-level pollution results for hourly average  $\text{NO}_2$  and  $\text{O}_3$ , and for daily average  $\text{PM}_{10}$  and  $\text{PM}_{2.5}$ , were extracted from the nearest grid point to each of the monitoring sites on the inner grid (1.5-km spacing), and are summarised for Robust Highest Concentration (RHC) in Figures 8.2 and 8.3 respectively. These results show that TAPM simulations of the extreme concentrations are very good for all species, although data at only three sites were available for  $\text{PM}_{2.5}$ .

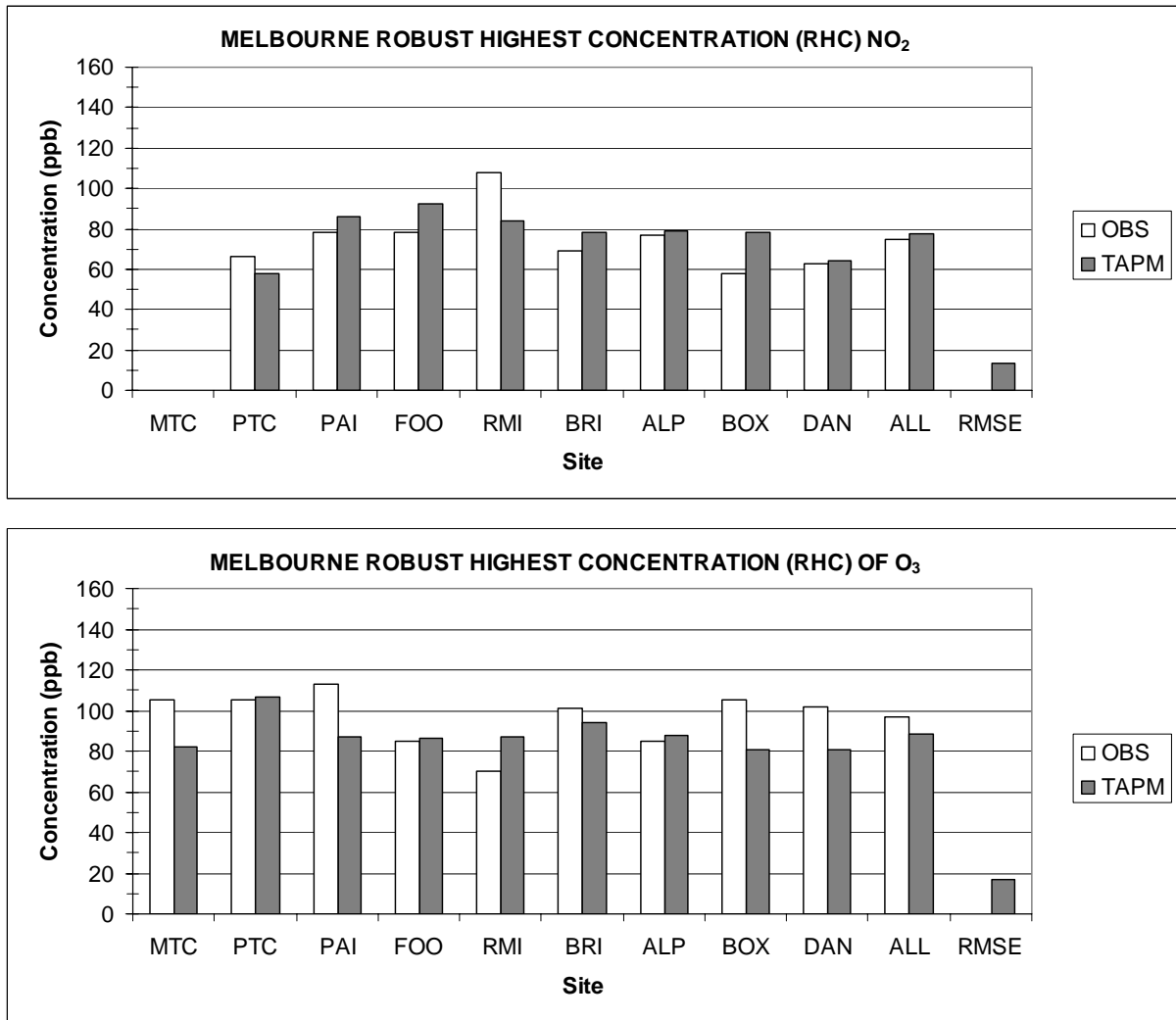


Figure 8.2. Nitrogen dioxide (top) and ozone (bottom) Robust Highest Concentration (RHC) values for each monitoring site and for the average over all sites, for TAPM.

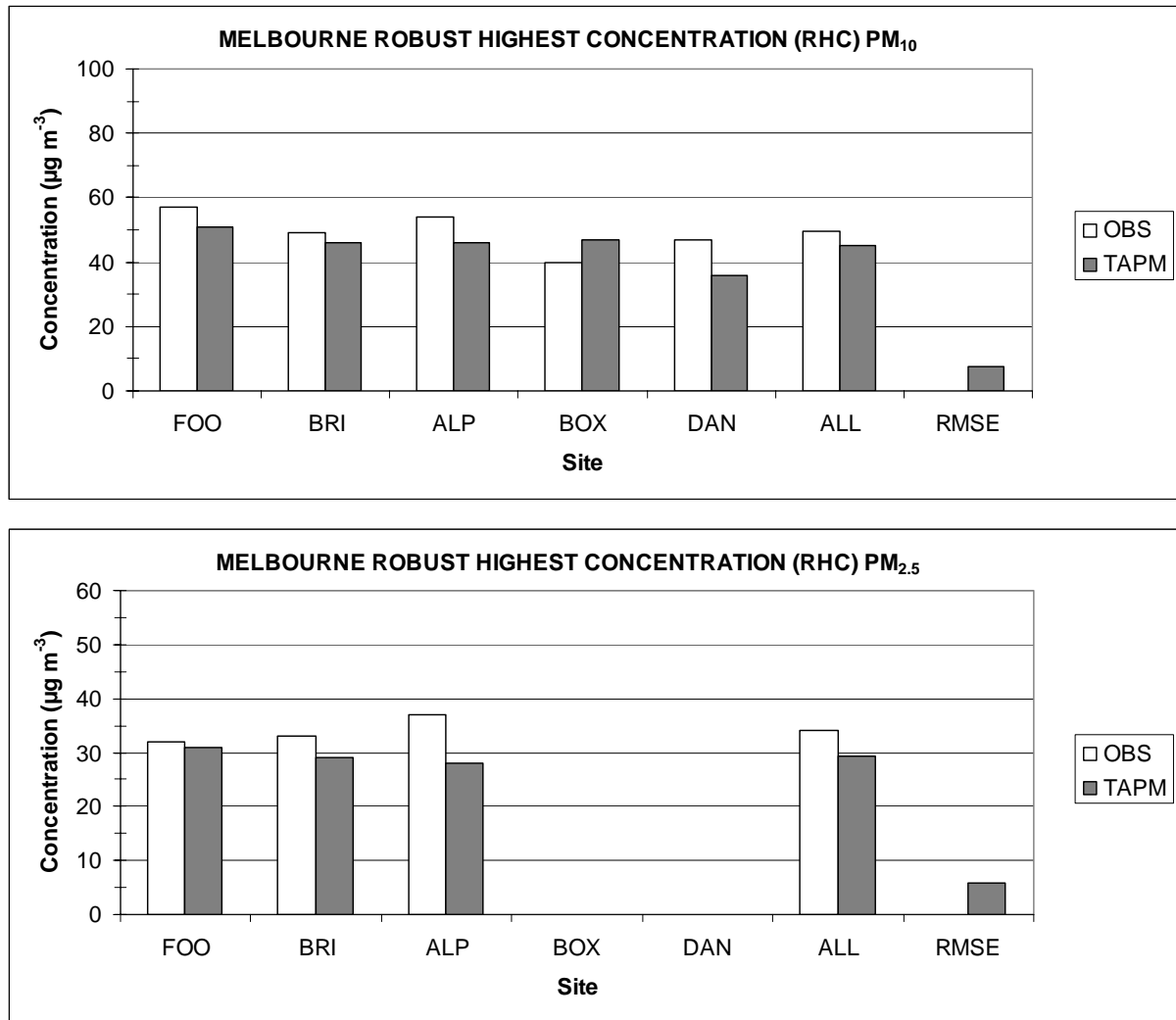


Figure 8.3. PM<sub>10</sub> (top) and PM<sub>2.5</sub> (bottom) Robust Highest Concentration (RHC) values for each monitoring site and for the average over all sites, for TAPM.

## **Acknowledgments**

Thanks to:

- US Geological Survey, Earth Resources Observation Systems (EROS) Data Center Distributed Active Archive Center (EDC DAAC), for access to the global terrain and land-use datasets;
- Geoscience Australia and CSIRO Wildlife and Ecology for access to the Australian terrain and land-use datasets;
- Australian Bureau of Meteorology for the LAPS/GASP synoptic meteorology datasets;
- US National Center for Atmospheric Research (NCAR) for access to the global sea-surface temperature dataset;
- National Centers for Environmental Prediction (NCEP)/National Center for Atmospheric Research (NCAR) for access to the synoptic reanalysis data used for the Kincaid and Indianapolis tracer studies, and to Mark Collier for help with processing this data into a form suitable for use by TAPM;
- those organisations involved with developing the Kincaid and Indianapolis tracer datasets in the Model Validation Kit, as part of the European initiative on “Harmonisation within Atmospheric Dispersion Modelling for Regulatory Purposes”.
- Barry Knight of Alcoa Anglesea power station for providing access to Anglesea emission and monitoring data, and for John Hill of Ecoplan for his major contribution to modelling emissions, meteorology and dispersion in the Anglesea region;
- Adrian Blockley and Ken Rayner of the Department of the Environment (DoE) and the Kwinana Industries Council for access to the Kwinana emissions data and air monitoring data, and for provision of the DISPMOD results for Kwinana;
- Bryn McDougall of Western Mining Corporation for providing the Kalgoorlie tower and SODAR data;
- Adrian Blockley of the Department of the Environment (DoE) and Philip Brace of Woodside for access to the Pilbara emissions data and air monitoring data;
- EPA Victoria for allowing access to the Melbourne emissions inventory and for providing meteorology and air pollution data from their air monitoring network, and to Sunhee Lee for extracting the inventory from the AAQFS in an appropriate form.

## References

- Bowne N. E., Londergan R. J., Murray D. R. and Borenstein H. S. (1983). 'Overview, results and conclusions for the EPRI plume model validation project: plain site', EPRI Report EA-3074, EPRI, Palo Alto, CA 94304.
- Cox W. and Tikvart J. (1990). 'A statistical procedure for determining the best performing air quality simulation', *Atmos. Environ.*, **24A**, 2387-2395.
- Deardorff J. W., and Willis G.E. (1984). 'Ground level concentration fluctuations from a buoyant and a non-buoyant source within a laboratory convective mixed layer', *Atmos. Environ.*, **18**, 1297-1309.
- Edwards M. , Hurley P. and Physick W. (2004). 'Verification of TAPM meteorological predictions using SODAR data in the Kalgoorlie region', *Aust. Met. Mag.*, **53**, 29-37.
- Hanna S. (1989). 'Confidence limits for air quality model evaluations, as estimated by bootstrap and jackknife resampling methods', *Atmos. Environ.*, **23**, 1385-1398.
- Hill J. and Hurley P. (2003). 'The use of TAPM at Anglesea', *Proceedings of the National Clean Air Conference of CASANZ*, Newcastle, Australia, 23-27 November 2003.
- Hurley P. (2005). 'The Air Pollution Model (TAPM) Version 3. Part 1: Technical Description', CSIRO Atmospheric Research Technical Paper No. 71. 54 pp.
- Hurley P., Blockley A., and Rayner K. (2001). 'Verification of a prognostic meteorological and air pollution model for year-long predictions in the Kwinana region of Western Australia', *Atmos. Environ.*, **35**, 1871-1880.
- Hurley P., Manins P., Lee S., Boyle R., Ng Y. and Dewundege P. (2003a). 'Year-long, high-resolution, urban airshed modelling: Verification of TAPM predictions of smog and particles in Melbourne, Australia', *Atmos. Environ.*, **37**, 1899-1910.
- Hurley P., Physick W., Cope M., Borgas M., Brace P. (2003b). 'An evaluation of TAPM for photochemical smog applications in the Pilbara region of WA', *Proceedings of the National Clean Air Conference of CASANZ*, Newcastle, Australia, 23-27 November 2003.
- Hurley P. and Luhar A. (2005). 'An evaluation and inter-comparison of AUSPLUME, CALPUFF and TAPM. Part I: The Kincaid and Indianapolis field datasets', *Clean Air*, **39**, 39-45.
- Hurley P., Hill J., and Blockley A. (2005a). 'An evaluation and inter-comparison of AUSPLUME, CALPUFF and TAPM. Part II: Anglesea and Kwinana annual datasets', *Clean Air*, **39**, 46-51.
- Hurley P., Physick W. and Luhar A. (2005b). 'TAPM – A practical approach to prognostic meteorological and air pollution modelling', *Environmental Modelling & Software*, **20**, 737-752.
- Kalnay E. et al. (1996). 'The NCEP/NCAR 40-Year Reanalysis Project', *Bull. Amer. Meteorol. Soc.*, **77**, 437-71.
- Luhar A., and Hurley P. (2003). 'Evaluation of TAPM, a prognostic meteorological and air pollution model, using urban and rural point-source data', *Atmos. Environ.*, **37**, 2795-2810.
- Olesen H. R. (1995). 'The model validation exercise at Mol: overview of results', *Int. J. Environ. Pollut.* **5**, 761-84.

- Pielke R.A. (1984). 'Mesoscale Meteorological modelling', Academic Press, Orlando, 612 pp.
- Physick, W.L., Rayner, K.N., Mountford, P., and Edwards M. (2004). 'Observations and modelling of dispersion meteorology in the Pilbara region'. *Aust. Met. Mag.*, **53**, 175-187.
- Puri K., Dietachmayer G.S., Mills G.A., Davidson N.E., Bowen R.A., and Logan L.W. (1998). 'The BMRC Limited Area Prediction System, LAPS', *Aus. Met. Mag.*, **47**, 203-223.
- Rayner K. (1998). 'A model-based sulfur dioxide control policy for the Kwinana industrial region', *Proceedings of the 11th Clean Air and Environment Conference*, Durban, South Africa, 13-18 September, 1998.
- Rayner K. (2000). 'Improvements in the coastal dispersion model DISPMOD', *Proceedings of the 15th International Clean Air and Environment Conference*, Sydney, Australia, 26-30 November 2000.
- Schulman L., Strimaitis D. and Scire J. (2000). 'Development and evaluation of the PRIME plume rise and building downwash model', *J. Air & Waste Manage. Assoc.*, **50**, 378-390.
- Thompson R. (1993). 'Building Amplification factors for sources near buildings: A wind-tunnel study', *Atmos. Environ.*, **27A**, 2313-2325.
- TRC (1986). Urban Power Plant Plume Studies, EPRI Report EA-5468, EPRI, 3412 Hillview Ave, Palo Alto, CA 94304.
- Willmott C.J. (1981). 'On the Validation of Models', *Phys. Geography*, **2**, 184-194.

## APPENDIX

The statistics used to measure meteorological model performance in this paper are based on those used by Willmott (1981) and Pielke (1984), as described below.

Predicted Mean  $P_{mean} = \sum_{i=1}^N P_i$ , where  $P_i$  are the predictions.

Observed Mean  $O_{mean} = \sum_{i=1}^N O_i$ , where  $O_i$  are the observations.

Predicted Standard Deviation  $P_{std} = \sqrt{\frac{1}{N-1} \sum_{i=1}^N (P_i - P_{mean})^2}$ .

Observed Standard Deviation  $O_{std} = \sqrt{\frac{1}{N-1} \sum_{i=1}^N (O_i - O_{mean})^2}$ .

Pearson Correlation Coefficient  $r = \frac{N \left( \sum_{i=1}^N O_i P_i \right) - \left( \sum_{i=1}^N O_i \right) \left( \sum_{i=1}^N P_i \right)}{\sqrt{\left[ N \left( \sum_{i=1}^N O_i^2 \right) - \left( \sum_{i=1}^N O_i \right)^2 \right] \left[ N \left( \sum_{i=1}^N P_i^2 \right) - \left( \sum_{i=1}^N P_i \right)^2 \right]}}$ .

Root Mean Square Error  $RMSE = \sqrt{\frac{1}{N} \sum_{i=1}^N (P_i - O_i)^2}$ .

Systematic Root Mean Square Error  $RMSE_S = \sqrt{\frac{1}{N} \sum_{i=1}^N (\hat{P}_i - O_i)^2}$ .

Unsystematic Root Mean Square Error  $RMSE_U = \sqrt{\frac{1}{N} \sum_{i=1}^N (\hat{P}_i - P_i)^2}$ .

Index of Agreement  $IOA = 1 - \frac{\sum_{i=1}^N (P_i - O_i)^2}{\sum_{i=1}^N (|P_i - O_{mean}| + |O_i - O_{mean}|)^2}$ .

Measures of Skill  $SKILL_E = \frac{RMSE_U}{O_{std}}$ ,  $SKILL_V = \frac{P_{std}}{O_{std}}$  and  $SKILL_R = \frac{RMSE}{O_{std}}$ .

Note that  $N$  is the number of observations and  $\hat{P}_i = a + bO_i$  is the linear regression fitted formula with intercept ( $a$ ) and slope ( $b$ ).

The Robust Highest Concentration  $RHC = C(R) + (\bar{C} - C(R)) \ln((3R-1)/2)$  pollution statistic is from Cox and Tikvart (1990), with  $C(R)$  the  $R^{th}$  highest concentration and  $\bar{C}$  the mean of the top  $R-1$  concentrations. The value of  $R = 11$  is used here so that  $\bar{C}$  is the average of the top-ten concentrations, which is an accepted statistic for evaluation of model performance (Hanna, 1989). The RHC is preferred to the actual peak value because it mitigates the undesirable influence of unusual events, while still representing the magnitude of the maximum concentration (unlike percentiles or averages over the top-percentiles). The statistical performance measures used here for pollution with the Kincaid and Indianapolis datasets are the same as those used by Olesen (1995) in the Model Validation Kit.